Investigating the Anti-Cancer Effects of Small Molecule MEI-1 as a Potential MDM2 Inhibitor

Viktoria Katarina Ilić

A Thesis Submitted to the Faculty of Graduate Studies in Partial Fulfilment of the Requirements for the Degree of

Master of Science

Graduate Program in Biology
York University
Toronto, Ontario

September 2020

Abstract

MDM2 is an oncogenic E3 ligase found to be overexpressed in a number of human cancers, leading to poor prognosis. MDM2 overexpression inhibits the function of the tumour suppressor p53, which ubiquitinates p53 and tags it for proteasomal degradation. MDM2 also exhibits p53-independent oncogenic activities through targeting other tumour suppressor proteins, such as Foxo3a and Rb. Thus, a preferred strategy in anti-cancer therapeutic development is to inhibit MDM2 in cancer cells. A small molecule MEI-1 was identified through *in silico* screening targeting the MDM2 catalytic RING domain. The purpose of this project was to explore the anti-cancer effects of MEI-1 in a number of tested cancer lines including leukemia, breast carcinoma, osteosarcoma, and colorectal cancers.

Using biochemical and cellular assays, MEI-1 was found to induce apoptosis and inhibit MDM2 E3 ligase activity in leukemia and colorectal cancer cell lines. MEI-1 was shown to block MDM2-mediated ubiquitination and de-stabilize MDM2/MDMX, causing p53 stabilization and activation. Additionally, MEI-1 was shown to affect the stability of Foxo3a and Rb as both were reported to be MDM2 E3 ligase substrates. Lastly, MEI-1 was shown to physically bind with the recombinant MDM2: MDMX RING domain heterodimer using Biolayer Interferometry technology. These results provide biochemical and cellular evidence suggesting MEI-1 is a promising small molecule with anti-cancer effects through targeting MDM2. This study also reveals that inhibition of MDM2 through disrupting the MDM2:MDMX heterodimer could be a plausible approach for the development of MDM2 inhibitors as potential anti-cancer therapeutic agents.

Acknowledgments

I would like to express my sincere gratitude to my supervisor, **Dr. Yi Sheng**, for mentoring me and giving me a chance to work in her lab. Your support and encouragement has helped me become the scientist and critical thinker I am today.

Thank you to my advisor, **Dr. Chun Peng**, for providing constructive feedback and helpful suggestions to better my project. Your time and support will always be appreciated.

Thank you to **Gaby**, who became like a sister to me during my time at York. Your optimism and good nature never fails to amaze me. We've shared so many fun memories together and I look forward to sharing many more years of friendship.

Thank you to **David** for your friendship throughout the years. Your guidance and wisdom in laboratory techniques, your constant support and your enthusiasm for science continues to inspire me. I cannot wait to see what scientific discoveries you make in your career.

To my fellow lab members in the Sheng lab: **Gaby, Rahima, Greta, Milena, Miguel, Ernest, Chetna,** and **Wendy**. It was a joy working alongside and getting to know you all.

I also want to thank everyone at LSB for the good times. **Kyra, Christina, Vu Hong, Mohamed, Anna, Helen, Marjan, Farnaz, Paige, Nicholas** and previous students at LSB who made coming to the lab fun. I will cherish our memories forever!

I would also like to thank **Dr. Nicole Nivillac**. I had the privilege of being a Teaching Assistant for her course. I will always remember Dr. Nivillac's kindness and openness to discussion, and I hope to echo this positive attitude in my future career endeavors.

Thank you to my family, my Kuma Nadja, and my friends for believing in me when I did not believe in myself. Thank you to my parents, Ljiljana and Sladjan, for instilling courage and stubbornness in me and giving me strength to carry on in difficult times. Thank you to my deka, Tomislav, who continues to support my goals and dreams. Thank you to my uncle Dejan and aunt Milana for supporting me throughout this journey. Adrijana and Elijana, you both light up my life immensely. I would not be the ambitious and passionate person that I am today if it were not for you all. Each of you played a pivotal role throughout my M.Sc. journey, and for that I am forever grateful.

Last but certainly not least, I dedicate this thesis to my guardian angel, Nana. I know that she is proud of the person that I have become and is smiling down at me from Heaven. Nana, you are always in my heart.

Table of Contents

List of Tables

Chapter 2

Appendix

List of Figures

Chapter 1

Chapter 3

Abbreviations

AML-2	Acute Myeloid Leukemia 2 p53 wild type cell line
APAF-1	Apoptotic Protease Activating Factor-1
ATP	Adenosine Triphosphate
Bax	Bcl-2-like protein 4
BCA	Bicinchoninic Acid
BCL-2	B-cell Lymphoma 2
BJ-FB	BJ normal fibroblast cell line
BLI	Biolayer Interferometry
BSA	Bovine Serum Albumin
Casp-9	Caspase 9
CDK	Cyclin-dependent Kinase
CRL4	Cullin Ring E3 Ligase 4
DHFR	Dihydrofolate Reductase
DMSO	Dimethyl Sulfoxide
E1	Ubiquitin-activating Enzyme
E2	Ubiquitin-conjugating Enzyme
E2F	E2 Factor
E3	Ubiquitin Ligase Enzyme
ECL	Enhanced Chemiluminescence
FBS	Fetal Bovine Serum
Foxo3a	Forkhead Box Protein O3A
GAPDH	Glyceraldehyde 3-Phosphate Dehydrogenase
HCT116 -/-	Human Colorectal Carcinoma p53 null Cell line
HCT116 +/+	Human Colorectal Carcinoma p53 wild type Cell line
HECT	Homologous to the E6-AP Carboxyl Terminus
HL-60	Acute Myeloid Leukemia p53 null cell line
HLI373	HDM2 Ligase Inhibitor 373
HLI98	HDM2 Ligase Inhibitor 98
HRP	Horseradish Peroxidase
IBR	In Between RING
IC_{50}	Half Maximal Inhibitory Concentration
IPTG	Isopropyl β- d-1-thiogalactopyranoside
K48	Lysine 48
MCF-7	Michigan Cancer Foundation-7 Breast Carcinoma Cell Line
MDM2	Mouse Double Minute 2 Homolog
MDMX	Mouse Double Minute X Homolog
MEI-1	MDM2 E3 Ligase Inhibitor-1
MLKL	Mixed Lineage Kinase Domain-like

Nbs1	Nibrin
NEM	N-Ethylmaleimide
NES	Nuclear Export Signal
NLS	Nuclear Localization Sequence
NMR	Nuclear Magnetic Resonance
Noxa	Phorbol-12-myristate-13-acetate-induced protein 1
PARP	Poly-ADP Ribose Polymerase
PBS	Phosphate Buffered Saline
PcG	Polycomb Group
PMSF	Phenylmethylsulfonyl fluoride
PRC2	Polycomb Repressor Complex 2
PROTAC	Proteolysis-Targeting Chimeras
PUMA	p53 Upregulated Modulator of Apoptosis
PVDF	Polyvinylidene difluoride
Ras/ERK/AKT	Extracellular signal-regulated kinase/Protein kinase B pathway
Rb	Retinoblastoma Protein
RBR	RING-between RING-RING
RING	Really Interesting New Gene
RIPA	Radioimmunoprecipitation Assay
RIPK3	Receptor-interacting serine/threonine-protein kinase 3
SDS	Sodium Dodecyl Sulfate
SDS-PAGE	Sodium Dodecyl Sulfate–Polyacrylamide Gel Electrophoresis
Ser15	Serine 15
Ser20	Serine 20
TBST	Phosphate buffered saline with Tween-20
Thr18	Threonine 18
U2OS	Human Bone Osteosarcoma Epithelial cells
UPS	Ubiquitin Proteasome System
WT	Wild type

Chapter 1: Introduction

1.1. The Discovery of MDM2

MDM2 (Murine Double Minute 2), also known as HDM2 in humans, is an oncogenic RING E3 ubiquitin ligase that serves as a negative regulator of tumour suppressor p53 (Haupt et al., 1997; Honda et al., 1997; Kubbutat et al., 1997). The primary role of MDM2 has been shown to inhibit the activity of p53 and keep p53 in check in cells (Momand et al., 1992; reviewed in: Momand et al., 2011). MDM2 was initially identified as one of three genes (*MDM1*, *MDM2*, and *MDM3*) found to be overexpressed in the tumorigenic mouse cell line 3T3-DM (Fakharzadeh et al., 1991; reviewed in: Lozano & Iwakuma 2003). *MDM1, MDM2,* and *MDM3* genes were detected in double minutes, which are small extrachromosomal nuclear bodies that result from gene amplifications (reviewed in: Lozano & Iwakuma 2003; Momand et al., 2011). MDM2 amplification was also shown to occur in human cancer cells (reviewed in: Mendoza et al., 2014). Approximately 10-20% of human cancers have been reported to exhibit overexpression of MDM2 (Jones et al., 1998). MDM2 is commonly overexpressed in soft tissue sarcomas (~20%), osteosarcomas, esophageal carcinomas, and breast carcinomas (~15%) (Oliner et al., 1992; Momand et al., 1998; Burgess et al., 2016). Overexpression of MDM2 has been shown to lower p53 levels in cancer cells, inhibiting p53 function in DNA repair, senescence, cell cycle arrest and apoptosis, leading to tumorigenic transformation (reviewed in: Nakagawara & Ozaki, 2011). Thus, E3 ligase MDM2 has been under intensive study as a drug target for the development of novel anti-cancer therapeutics in cancer research.

1.2. MDM2 Protein Structure and Function

The *MDM2* gene is situated on human chromosome 12q14.3-q15, which encodes the protein MDM2 consisting of 491 amino acids in length and migrating at 90 kDa in an SDS-PAGE gel (reviewed in: Mendoza et al., 2014). MDM2 contains several functional domains

(Figure 1.1A). The N-terminus of MDM2 contains a p53-binding domain. Tumour suppressor p53 interacts with this domain, which results in the inhibition of p53 transcriptional activity (Kussie et al., 1996). The central region of MDM2 contains the nuclear localization sequence (NLS) and the nuclear export signal (NES), two motifs that are responsible for the shuttling of MDM2 between the nucleus and the cytoplasm (Muelmeester et al., 2003; O'Keefe et al., 2003). MDM2 also contains an acidic domain and a zinc finger domain. Both domains were shown to facilitate MDM2 contact with various ribosomal proteins (Kawai et al., 2003; Lindström et al., 2007). Lastly, MDM2 contains a RING (Really Interesting New Gene) finger domain at its C-terminus. The MDM2 RING finger domain is responsible for its E3 ubiquitin ligase activity, which leads to substrate polyubiquitination (Yasuda & Honda, 2000; Poyurovsky et al., 2007).

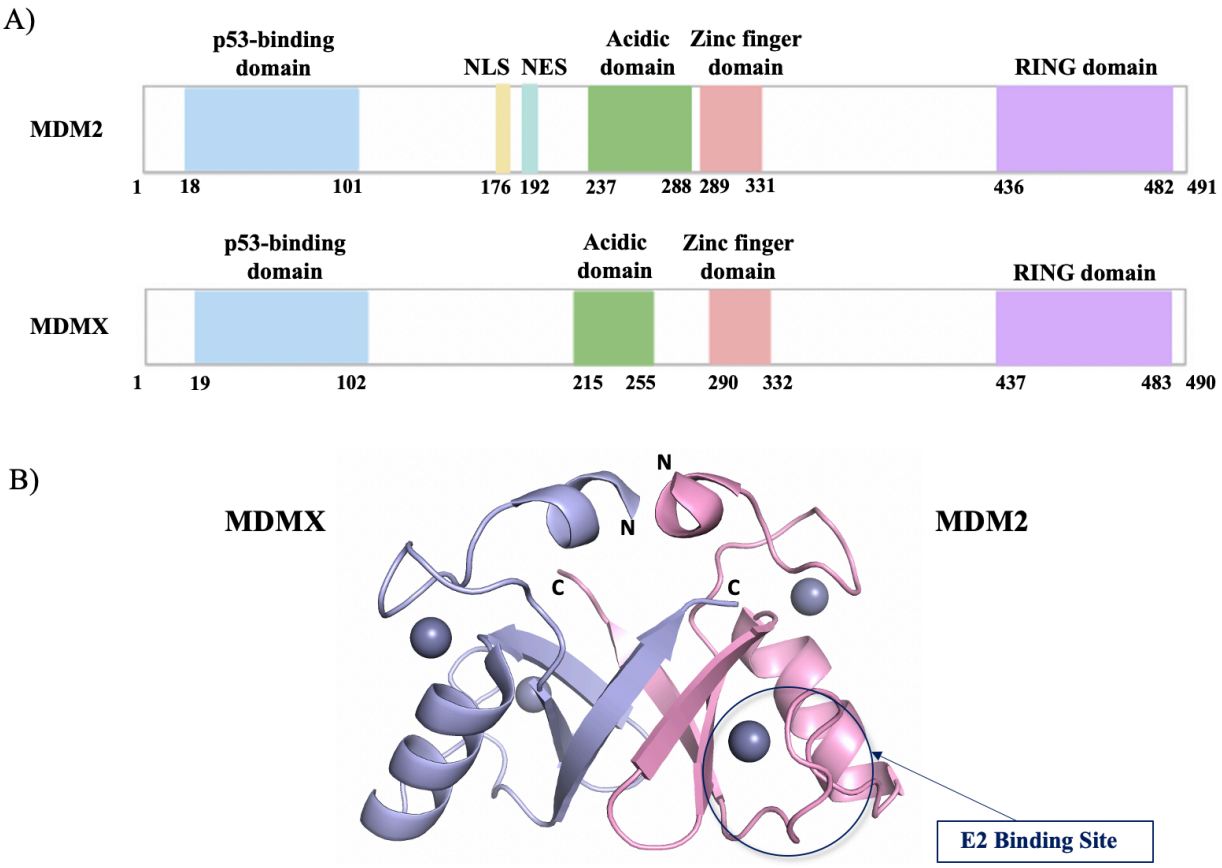

Figure 1.1 (A-B) MDM2 and MDMX. (A) Protein domain structures of MDM2 and MDMX, respectively. Both MDM2 and MDMX contain an N-terminal p53-binding domain (blue), a central acidic domain (green), a zinc finger domain (light pink), and a C-terminal RING domain (purple). MDM2 possesses a nuclear localization signal (NLS, yellow) and the nuclear export sequence (NES, teal). Numbers represent residue positions. (B) Crystal structure of the MDM2: MDMX RING domain heterodimer. The MDM2 RING is depicted in pink and the MDMX RING is shown in purple. MDM2 E2 binding is located at the C-terminus and is circled in navy. Zinc ions are represented as purple spheres. Crystal structure was generated using Pymol software.

1.3. MDM2 is a RING finger Domain E3 Ubiquitin Ligase

MDM2 is an E3 ubiquitin ligase capable of self-ubiquitination as well as ubiquitination of specific substrate proteins (Ciechanover & Bie, 2011; Yang & Ranaweera, 2013). MDM2 E3 ligase activity is mediated by the RING domain, which catalyzes the attachment of a polyubiquitin chain onto its substrate proteins (Fang et al., 2000; Lozano & Iwakuma, 2003). Ubiquitin is a small protein of 8.5 kDa in size and can be covalently conjugated to substrate proteins in forms of mono-ubiquitination or poly-ubiquitination (Callis, J., 2014). Protein modification by covalent conjugation of ubiquitin could change the function and fate of the modified protein in different ways, such as signalling for the degradation of ubiquitin-tagged proteins by the proteasome, altering subcellular localization, or inducing/inhibiting protein-protein interactions (reviewed in: Hall & Prives, 1999; Petrenko & Moll, 2003).

The elegant process of ubiquitination involves a cascade of E1 ubiquitin-activating enzyme, E2 ubiquitin-conjugating enzymes and E3 ubiquitin ligases, all of which play vital roles in this process (Ciechanover, A., 1994; Maki et al., 1996). Ubiquitination begins with E1, an ATP dependent enzyme that binds, activates and forms a thioester intermediate with ubiquitin (Figure 1.2). E2 transfers ubiquitin from E1 to its own catalytic cysteine residue. E3 transfers ubiquitin from E2 to the lysine residue of the targeted protein, forming an isopeptide bond between the lysine residue and ubiquitin (Hochstrasser, M., 1995; Scheffner et al., 1995; Kauffman & Adams, 2004; Chen et al., 2011; Stewart et al., 2016). Ubiquitin contains seven lysine residues. Additional ubiquitin molecules could be attached to any of the seven lysines to form linkage specific polyubiquitin chains. The 26S proteasome recognizes the substrate proteins with Lys48 linked poly-ubiquitin and degrades the proteins into peptides (Figure 1.1) (Schrader et al., 2009; Nathan & Grice, 2016).

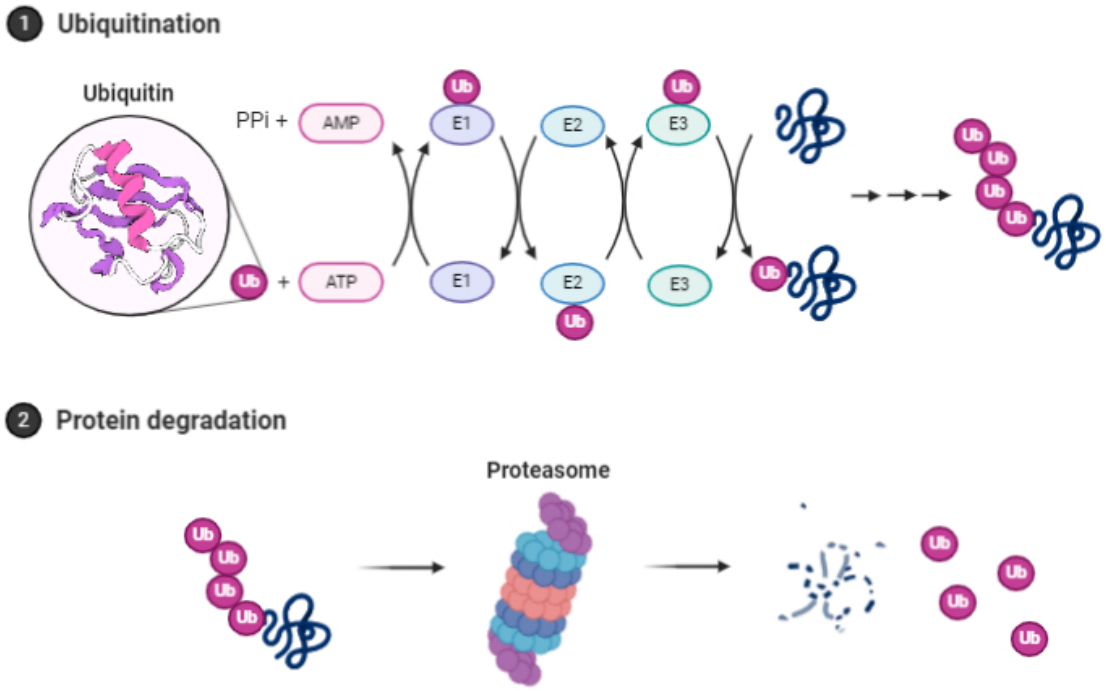

Figure 1.2 The Ubiquitin Proteasome System (UPS). Step 1: Ubiquitin is activated by ATP with E1 (ubiquitin-activating enzyme), followed by ubiquitin transfer to E2 (ubiquitin-conjugating enzyme). E3 ligases are responsible for transferring ubiquitin molecule from E2 and conjugation of ubiquitin with the target protein. Step 2: Depiction of protein degradation of the polyubiquitinated substrate protein into peptides by the proteasome (The image was generated using Biorender).

The human genome encodes hundreds of single polypeptide E3 ubiquitin ligases, which can be classified into HECT (Homologous to the E6-AP Carboxyl Terminus) domain E3 ligases, the RING (Really Interesting New Gene) finger domain E3 ligases, the U box domain E3 ligases, and the RBR (RING between RING) E3 ligases (reviewed in: Robinson & Ardley, 2005; Spratt et al., 2014). For substrate ubiquitination, the HECT domain E3 ligases require a cysteine residue to form the ubiquitin catalytic intermediate during ubiquitin transfer. The RING finger domain E3s are zinc-binding proteins, on the other hand, that do not form a ubiquitin catalytic intermediate (Metzger et al., 2012). Instead, the RING domain serves as a scaffold to mediate the transfer of ubiquitin directly from E2 to the substrate proteins. The U box domain E3 shows similar structural topologies to the RING domain but lacks zinc coordination and mediates the substrate ubiquitination using a mechanism similar to the RING domain. The RBR domain E3s are unique, since each RBR has two RING domains (RING1 and RING2) and is divided by the IBR (in between RING) domain. The RBR domain functions mechanistically similar to the HECT domain as it also catalyzes the transfer of ubiquitin with a catalytic intermediate (Walden & Morreale, 2016).

MDM2 is a RING domain containing E3 ligase. The structure of the MDM2 RING domain contains two zinc cations that are coordinated by seven cysteines and one histidine (Metzger et al., 2012). This forms a “cross-brace” structure and facilitates E2 ubiquitin transfer (Moududee et al., 2018). The RING domain interacts with E2 and promotes ubiquitin ligation with the designated lysine residues on target proteins. Thus, the RING domain at the C-terminus of MDM2 functions as a catalytic centre to mediate the ubiquitination of its substrate proteins, such as p53.

MDM2 RING finger domain requires dimerization to form an active E3 ligase (Nomura et al., 2017). MDM2 RING domain dimerization can result in a homodimer of two MDM2 RING domains (MDM2: MDM2) or a heterodimer of MDM2 RING domain with MDMX RING domain (MDM2: MDMX). MDMX is the homologous protein of MDM2, which contains a conserved RING domain in its C-terminus. (Shvarts et al., 1997). The solution NMR structure of MDM2: MDM2 RING homodimer, solved by Kostic and colleagues, was depicted as a six stranded β-barrel structure and flanked with two α-helices on both sides, consisting of two stable β-β-α-β structures coordinated by Zn^{2+} ion (Kostic et al., 2006). The crystal structure of MDM2: MDMX RING domain heterodimer, determined by Linke et al. as (Figure 1.1B) (Linke et al., 2008), also showed a symmetrical β-barrel surrounded by two helices, a structural topology similar to that of MDM2: MDM2 RING homodimer. Both MDM2 and MDMX RING domain of the heterodimer adopt a β-β-α-β fold, with three β strands contributing to half of the β-barrel structure. The dimerization was mediated by the first β strand of MDMX with the last seven residues of MDM2 and the first β strand of MDM2 with the last seven residues of MDMX. Nomura and colleagues described the conserved E2 binding site of MDM2 to be a shallow groove on the surface of the MDM2 RING domain, between its α-helix and the second β strand (Nomura et al., 2017). As described above, MDMX plays a role in shaping the β-barrel structure and provides stability to the overall structure of MDM2: MDMX heterodimer. As a result, the formation of the MDM2: MDMX RING heterodimer seems to be favoured over MDM2 or MDMX homodimer formation. MDM2: MDMX heterodimer seems to lead to a stable complex and greater E3 ligase activity towards p53 (Linke et al., 2008).

1.4. MDMX, The Homologous Protein of MDM2

MDMX, also known as MDM4, is 490 amino acids in length (Marine & Jochemsen, 2005). As the homologous protein of MDM2, MDMX consists of a p53-binding domain at the N-terminus, an acidic domain and a zinc-finger domain in the centre, and a RING finger domain located at the C-terminus (Figure 1.1A) (Pazgier et al., 2009). The p53-binding domain and the RING finger domain appear to be structurally similar and highly conserved in both MDMX and MDM2 (Marine et al., 2007). However, the RING domain of MDMX does not possess intrinsic E3 ligase activity when forming a homodimer (Herman et al., 2011; Sheng & Egorova, 2014; Karni- Schmidt et al., 2016). Thus, MDMX functions primarily as the MDM2 heterodimer binding partner, which works together with MDM2 to inhibit p53 activity and function (Linke et al., 2008; Shadfan et al., 2012; Burgess et al., 2016).

Like MDM2, MDMX is also an oncogene frequently altered in human cancers (Tisato et al., 2017). MDMX overexpression has been found in many tumour types, including retinoblastoma, sarcomas, breast carcinomas, and glioblastomas (Danovi et al., 2004; Tisato et al., 2017). MDMX is capable of binding to the p53 transactivation domain and inhibits its transcriptional activity (Shvarts et al., 1996; Ghosh et al., 2003; Zhang et al., 2014). Since MDMX does not contain an NLS domain, the protein is unable to shuttle from the cytoplasm to the nucleus and requires MDM2 to elicit p53 suppressive function in the nucleus (Shadfan et al., 2012).

1.5. p53/ MDM2 Negative Feedback Loop

Previous studies have shown that the main function of MDM2 as a key negative regulator of p53 is to hinder p53 tumour suppressor activity (Levine, A.J., 1997; Wade et al., 2010; Momand et al., 2011). p53 is mutated or lost in approximately 50% of human cancers through *TP53* gene mutation and deletion (Olivier et al., 2010; Nakagawara & Ozaki, 2011; Perri et al., 2016). In cancers with the wildtype *TP53* gene, the p53 function is often suppressed by overexpression of its negative regulators, including MDM2 and MDMX. MDM2 and p53 form a negative feedback loop. As a primary E3 ligase for p53, MDM2 tags p53 for ubiquitination and facilitates its degradation (Lane & Picksley 1993; Wu et al., 1993; Petrenko & Moll, 2003). MDM2 also directly binds to the N-terminus of p53 protein and inhibits p53 transcriptional activity (Oliner et al., 1993; Wu et al., 1993). On the other hand, MDM2 is transcriptionally activated by p53 under DNA damage. Thus, the levels of p53 and MDM2 appear in an oscillation pattern in the cell (Gray & Proctor, 2008). The delicate balance between MDM2 and p53 levels is essential in determining p53 cellular activity.

Under normal conditions, p53 is maintained at basal levels and negatively regulated by MDM2 that keeps p53 levels in check, allowing cells to grow and proliferate. Upon DNA damage or genotoxic stresses, p53 is phosphorylated at the MDM2 binding site, including Ser15, Thr18, or Ser20, resulting in MDM2 dissociation, p53 activation and accumulation in the cell (reviewed in: Jiang et al., 2010). p53 serves as a G1/S and G2/M checkpoint in the cell cycle (Agarwal et al., 1995; Manfredi & Senturk, 2013). Mild DNA damage leads to p53 activation and cell cycle arrest through the transcriptional activation of target genes, including cyclin dependent kinase (CDK) inhibitor p21 and 14-3-3 protein. Both proteins participate in halting cell cycle progress and preventing cell division (Yang et al., 2003; Marine & Lozano, 2010;

Burgess et al., 2016). Severe DNA damage can result in p53 induced apoptosis by transactivating pro-apoptotic BCL-2 family genes such as Bax, PUMA (p53 upregulated modulator of apoptosis), APAF-1 (apoptotic protease activating factor 1) and Noxa, which initiate a cascade of events that lead to programmed cell death (Oda et al., 2000; Soengas et al., 2001; Vousden & Nakano, 2001; Haupt et al., 2003; Lowe & Fridman, 2003). This process begins with the release of cytochrome C from mitochondria, forming a complex with APAF-1. This complex, known as the apoptosome, recruits pro-caspase 9 and converts it into activated caspase-9. Caspase-9 triggers a caspase cascade, leading to the activation of the apoptosis executioner caspase-3. Caspase-3 cleaves cytosolic and nuclear proteins, such as PARP (Poly ADP-Ribose Polymerase), causing cell death to occur (Oliver et al., 1998; Haupt et al., 2003; reviewed in: Elmore, S., 2007). PARP, a nuclear enzyme responsible for Poly ADP-ribosylation of substrate proteins, catalyzes the transfer of ADP-ribose polymers onto itself and other nuclear proteins involved in the DNA repair process (Bouchard et al., 2003). Thus, cleaved PARP and cleaved caspase-9 serve as hallmarks of apoptosis.

Under cancerous conditions, the balance between p53 and MDM2 is disturbed. The overexpression of MDM2 can lead to the inhibition of p53 and tumorigenesis. Therefore, MDM2 has been a desired drug target for the development of anti-cancer therapeutics to restore p53 function and to induce apoptosis in carcinogenic cells.

1.6. p53-Independent Functions of MDM2

Increasing evidence suggests that MDM2 can promote tumorigenesis through p53-independent pathways. MDM2 overexpression has been associated with chromosomal abnormality and genomic instability (Bousken et al., 2008). Past research has demonstrated that MDM2 plays a role in chromatin remodeling and is directly involved in DNA repair through

interactions with nuclear proteins Nbs1 (Nibrin) and PRC2 (Polycomb Repressor Complex 2), respectively (Wienken et al., 2017; Egorova et al., 2020). Nbs1 has been shown to act in the repair of double strand DNA breaks while PRC2, from the PcG (polycomb group) family of proteins, partakes in modifying chromatin structure (Alt et al., 2005; Wienken et al., 2017). In addition, MDM2 serves as an E3 ligase and targets multiple p53-independent tumour suppressor proteins, including Rb (Retinoblastoma protein) and Foxo3a (Forkhead box O 3a) (Zhang el al., 2014).

The retinoblastoma protein, Rb, is another important tumour suppressor frequently deregulated in cancer cells (reviewed in: Zhu, L., 2005). Rb plays a crucial role in cell cycle inhibition and apoptosis. Rb forms a complex with a family of transcription factors, E2F, preventing transcription of growth promoting genes, including cyclin E and DHFR (Knudsen et al., 1999; reviewed in: Dean & Harbour, 2000). The mitogenic signals lead to Rb phosphorylation by cyclin D and cyclin dependent kinases (CDKs) and subsequent degradation by the proteasome, resulting in activation of E2F and cell proliferation (Alao, J.P., 2007). Thus, downregulation, including loss of Rb, can result in cell cycle deregulation and tumorigenesis (reviewed in: Giardano & Giacinti, 2006; Knudsen & Knudsen, 2008). It has been reported that MDM2 could directly ubiquitinate Rb and facilitate its degradation. MDM2 forms a complex with Rb and the interaction between MDM2 and Rb prevents Rb from binding to the E2F transcription factor (Xiao et al., 1995; Polager & Ginsberg, 2009). Thus, MDM2 overexpression can lead to the disruption of the Rb: E2F pathway, resulting in uncontrolled cell proliferation.

Foxo3a tumour suppressor protein plays a role in the regulation of the Ras/ERK/AKT pathway. The proliferating signal activates the Ras/ERK/AKT pathway, which downregulates Foxo3a activity through its phosphorylation to regulate cell proliferation and differentiation.

Once Foxo3a has been phosphorylated, it is exported from the nucleus and sent to the cytoplasm of the cell, forming a complex with 14-3-3 protein (reviewed in: Farhan et al., 2017). Foxo3a has been shown to be ubiquitinated by MDM2 and tagged for degradation by the proteasome (Liu et al., 2018). Similar to p53, Foxo3a responds to cellular stresses and upregulates genes that cause cell cycle arrest, DNA damage repair, or apoptosis (reviewed in: Zhang et al., 2011). Foxo3a serves as a target of MDM2 in the Ras/ERK/AKT pathway (Yang, J.W. et al., 2008; reviewed in: Yang, W. et al., 2008; Fu et al., 2009). Its association with MDM2 could result in Foxo3a inactivation and degradation. Therefore, overexpression of MDM2 could contribute to uncontrolled cellular proliferation and tumorigenesis through downregulation of Foxo3a.

1.7. Current MDM2 Inhibitors

MDM2 inhibitors are becoming promising cancer therapeutic agents because of their ability to block MDM2 tumorigenic activity in p53-dependent and p53-independent pathways. Current inhibitors of MDM2 have been developed by different approaches. One approach is to develop small molecule compounds downregulating the transcription of MDM2. One of such compounds is 25-OCH_3-PPD (20(S)-25-methoxyl-dammarane-3β, 12β, 20-triol), a naturally derived ginsenoside product which inhibits MDM2 transcription and decreases the MDM2 level in the cell. Another approach is to promote MDM2 degradation, as seen with PROTACs 32 (proteolysis-targeting chimeras), which tags MDM2 to CRL4 for degradation (Wang et al., 2012; Wang et al., 2019). The development of small molecules to dissociate the MDM2-p53 complex and inhibit the MDM2 E3 ligase are the other two promising strategies, which have been under extensive research and debate, and therefore will be reviewed in detail below (Figure 1.3).

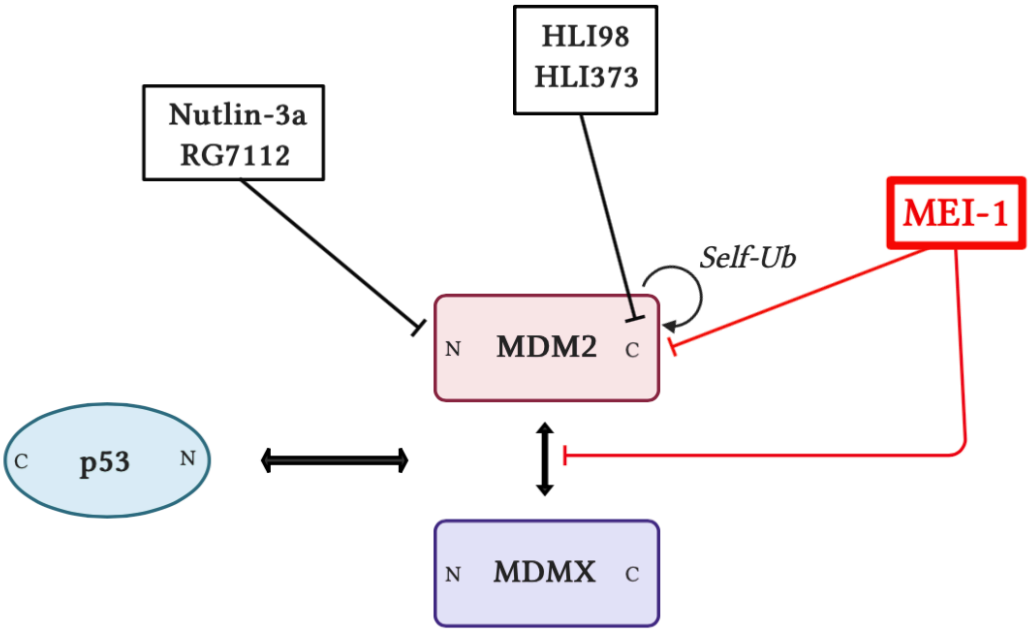

Figure 1.3 Schematic representation of current MDM2 inhibitors (Nutlin-3a and HLI198). Nutlin-3a binds to the N-terminus of MDM2 to dissociate the interaction between MDM2 and p53. HLI98 binds to MDM2 C-terminal RING domain to inhibit MDM2 E3 ligase activity. MEI-1small molecule was identified as an MDM2 E3 ligase inhibitor (Sheng lab, unpublished data) using a structure-based virtual screening strategy approach. MEI-1 may work through two mechanisms: inhibiting MDM2 E3 ligase activity and affecting MDM2: MDMX dimerization (figure adapted and modified from Burgess et al., 2016).

Targeting the MDM2-p53 interaction has shown some promising results for various human cancers. The pioneer small molecules developed to dissociate the MDM2-p53 complex are members of the nutlin family. Nutlin-3a, a cis-imidazoline compound, was the first small molecule MDM2 inhibitor discovered in 2004 by Vassilev and colleagues (Vassilev et al., 2004; Burgess et al., 2016; Gupta et al., 2019). Nutlin-3a binds to the p53-binding domain of MDM2, disrupting its interaction with p53, thus resulting in p53 stabilization and activation (Figure 1.3) (Marine & Lozano, 2010). Nutlin-3a has been shown to arrest proliferating cancer cells in the G1 and S stages of the cell cycle and induce apoptosis in several wild type p53 cell lines, including breast carcinoma, colorectal cancer, lung cancer, melanoma, and renal carcinoma cells (Gupta et al., 2019).

Recent studies demonstrated that MDM2 inhibition by nutlin-3a prevents DNA damage repair and causes synthetic toxicity with genotoxic agents independent of p53 (Verma et al., 2010; Carrillo et al., 2015). Off-target effects with prolonged exposure to nutlin-3a induced several incidences of p53 mutations (Aziz et al., 2011; Burgess et al., 2016). These off-target effects raised a concern that this family of MDM2 inhibitors may trigger carcinogenesis through promoting p53 mutations (Burgess et al., 2016). The clinical trial of nutlin analog, RG7112, showed that physiological on-site toxicities arose with the use of the drug, such as thrombocytopenia and neutropenia, and thus further development of RG7112 has been discontinued (Espadinha et al., 2018). Although a promising agent to antagonize the interaction between MDM2 and p53 and to restore the wild type p53 activity in cancerous cells, the negative impact of this class of MDM2 inhibitors warrants further investigation.

Alternative approaches have been taken by researchers to promote MDM2 auto-ubiquitination but inhibit MDM2 E3 ligase activity towards p53. Hdm2 Ligase Inhibitor

compounds HLI98 and second generation HLI373 were developed to inhibit MDM2-mediated p53 ubiquitination (Yang et al., 2005). Both HLI98 and HLI373 have been shown to possess high potency in the stabilization of p53 in several tumour cell lines by increasing p53 levels and inducing apoptosis (Kitagaki et al., 2008; Yang et al., 2009). These two small molecules inhibit MDM2 by targeting its C-terminal RING domain (Figure 1.3) (Chen et al., 2017). However, the development of HLI98 compound was discontinued due to its limited solubility and potency as well as its off-target inhibition of other cellular E3 ligases, which resulted in p53-independent cellular toxicity (Yang et al., 2005; Kitagaki et al., 2008). HLI373 was found to be more water soluble and exhibit better potency in the stabilization of p53 and MDM2, along with the ability to induce apoptosis, as compared to HLI98 (Kitagaki et al., 2008). Off-target effects and intrinsic toxicities of MDM2 inhibitor HLI373 have yet to be determined and require further investigation.

Although long-term effects of these MDM2 inhibitors have yet to be determined, both nutlin-3a and HLI98/HLI373 class compounds presented various issues. For example, the direct effect of nutlin-3a can stimulate MDM2 transcription and overexpression due to p53 stabilization, which could potentially induce genome instability and promote p53-independent tumorigenic activity of MDM2. On the other hand, HLI98/HLI373 inhibitors target the C-terminal RING domains and could lead to the stabilization of both p53 and MDM2, which prevents full activation of p53. Furthermore, HLI98/HLI373 targets the conserved RING domain E2 binding site and seem to have off-target effects on other E3 ligases in the cell. This inspired our lab to develop a novel MDM2 inhibitor by targeting the MDM2 RING domain to promote p53 stabilization and MDM2 de-stabilization.

1.8. The Discovery of MEI-1

Analysis of the crystal structural surface of the MDM2: MDMX RING heterodimer (PDB:2VJE) identified a ligand binding site that differed from the MDM2 conserved E2 binding sites targeted by HLI98/HLI373 compounds. This ligand binding site is situated at a location distant from the active site for MDM2 E2 binding, but close in proximity to the location of MDM2/MDMX dimerization. As MDM2/MDMX dimerization is important for the structural integrity of the RING domain, blocking this allosteric site might have an impact on MDM2/MDMX dimerization and overall structural stability. Using a computational screening and docking approach, a compound originating from a natural product was identified as one of the top-fitting chemicals to the targeted ligand binding site on the surface of the MDM2 RING domain, together with several other potential compounds (Figure 1.4). This compound was named MEI-1 (MDM2 E3 ligase Inhibitor 1). The preliminary data from the Sheng lab showed that MEI-1 inhibited MDM2 E3 ligase activity in a biochemical ubiquitination assay using recombinant MDM2 RING domain (Sheng Lab, unpublished data). In this assay, MEI-1 appeared to inhibit the E3 ligase activity of MDM2 more efficiently than the positive control, HLI373 (Sheng lab, unpublished). In addition, MEI-1 induced the stabilization of p53, resulting in cellular morphological changes and apoptosis in U2OS cells, suggesting that MEI-1 possesses an anti-cancer effect through inhibition of MDM2 (Sheng lab, unpublished).

The chemical name for MEI-1 is Hinokiflavone, also known as 4', 6''- O-Biapigenin derived from a natural product, (PubChem CID: 5281627) belonging to a bioflavonoid family (Figure 1.4A). Hinokiflavone has a molecular weight of 538.5 g/mol and its molecular formula is $C_{30}H_{18}O_{10}$. Hinokiflavone is a highly stable small molecule which could be isolated from several plants, including *Selaginella tamariscina*, *Juiperus phoenica*, and *Rhus succedanea*. Several

reports have shown Hinokiflavone has anti-tumour properties. Hinokiflavone was shown to induce apoptosis and inhibit migration and invasion of carcinogenic cells in colorectal, oral, melanoma and breast cancers (Yang et al., 2018; Zhou et al., 2018;Huang et al., 2019). Moreover, this compound has exhibited low cytotoxicity in non-carcinogenic cells (Huang et al., 2019). Based on these previous studies, Hinokiflavone has the potential to be developed as an anti-cancer therapeutic agent but the mechanism of its anti-cancer effect remains unknown.

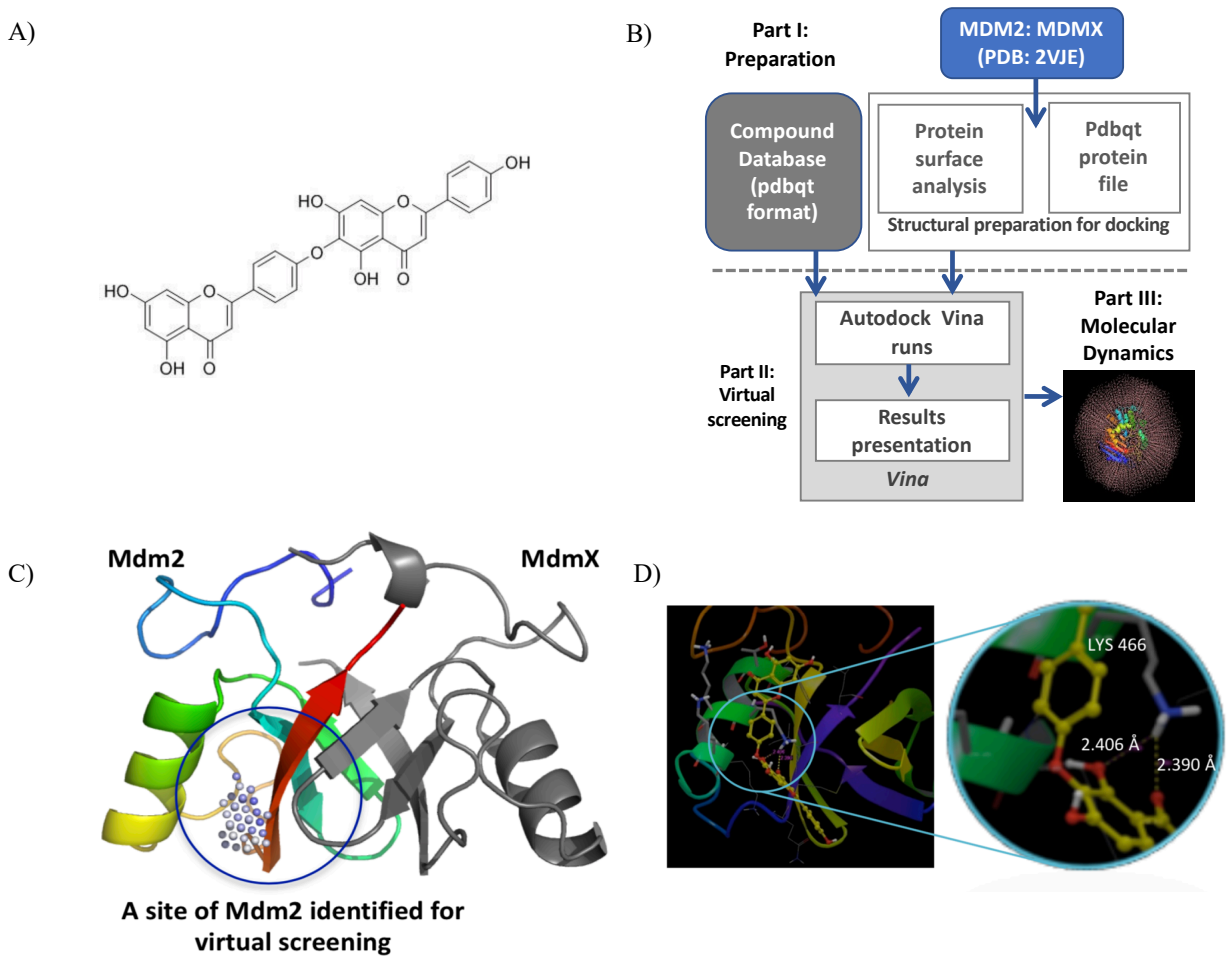

Figure 1.4 (A-D) MEI-1 identified through computational and docking approach. (A) Chemical structure of Hinokiflavone, represented as MEI-1 in this study. (B) Virtual screening workflow used for MDM2: MDMX RING domain heterodimer. MEI-1 was identified by virtual screening from 200,000 natural compounds targeting the allosteric site on the surface of MDM2: MDMX RING domain heterodimer (C). Crystal structure of the MDM2: MDMX domain heterodimer (PDB: 2VJE) used for virtual screening. MDM2 and MDMX are shown in rainbow and grey, respectively. Circled binding site is proposed to be the allosteric site, distant from the conserved E2-binding site, but close to the dimerization surface of the MDM2: MDMX RING domain. This site was used for virtual screening. (D). MEI-1 was docked onto MDM2 RING domain at the allosteric site. The enlarged view shows putative interactions between MDM2 RING Lys466 (shown in sticks) and the compound (shown in spheres and sticks).

1.9. The Rationale, Hypothesis and Objective of the Project

MDM2 overexpression has been associated with poor prognosis of several human carcinomas. MDM2 gene amplification and protein overexpression were shown to inhibit p53 tumour suppressive function, leading to malignant transformation. Additionally, past studies have shown that MDM2 caused genome instability and presented oncogenic activity through ubiquitination of other p53-independent proteins, such as Foxo3a and Rb. Therefore, MDM2 overexpression is considered a poor prognostic factor in human malignancies and a preferred drug target in anti-cancer therapeutic development.

Although targeting MDM2 E3 ligase as a therapeutic strategy is an attractive approach, no successful MDM2 inhibitors are presently available. Nutlin family 3 analogs could promote p53 stabilization but fail to prevent MDM2 accumulation in the cell. Currently available MDM2 RING domain inhibitors, HLI compounds, displayed cytotoxicity to carcinogenic cells but resulted in detrimental off-target effects. Therefore, a plausible and desired approach is to promote MDM2 de-stabilization by targeting the MDM2 RING domain. Targeting the MDM2 RING domain could also inhibit MDM2-mediated ubiquitination.

MEI-1, an MDM2 inhibitor, was identified using a virtual screening from a library of natural compounds with the potential ability to bind to the MDM2 RING domain and to target its dimerization site. Previous biochemical studies conducted by the Sheng lab have shown that MEI-1 indeed inhibited MDM2 E3 ligase activity (Sheng lab, unpublished data). MEI-1 treatment could stabilize p53 and induce apoptosis in the U2OS osteosarcoma cell line. The overarching goal of this project is to validate the anti-cancer effect of MEI-1 as an MDM2 inhibitor. The proposed hypothesis is that MEI-1 could inhibit MDM2-mediated substrate ubiquitination and de-stabilize MDM2 through its effect on MDM2 dimerization.

In this research project, the interaction of MEI-1 with MDM2: MDMX RING heterodimer and the effects of MEI-1 on p53-dependent and p53-independent substrates were examined using biochemical techniques. Several cancer cell lines, including p53 wild type and p53 null leukemia and colorectal cancer cells, were used to evaluate the effect of MEI-1 as an MDM2 inhibitor. A biochemical assay was performed to investigate the interaction between MEI-1 and the MDM2 RING domain to validate MEI-1 as an allosteric binder for MDM2 inhibition.

The following four aims were thoroughly investigated in this study to evaluate the anti-cancer effect of MEI-1 as an MDM2 inhibitor.

Aim 1. *Assessment of cell viability in cancer cell lines and normal fibroblast cells upon MEI-1 treatment.*

Carcinogenic cell lines, including leukemia, colorectal cancer, osteosarcoma and breast carcinoma cells, as well as BJ normal fibroblasts, were treated with MEI-1 to explore possible anti-cancer effects of MEI-1 and its cytotoxicity in cancerous versus normal cells.

Aim 2*. Investigation of the effect of MEI-1 in MDM2-mediated ubiquitination in p53 wild type and p53 null leukemia cell lines, respectively.*

Using a cellular ubiquitination assay, MDM2-mediated p53 ubiquitination and/or MDM2 auto-ubiquitination were evaluated in p53 wild type and p53 null leukemia cell lines to determine the effect of MEI-1 on MDM2 E3 ligase activity.

***Aim 3**. Characterization of the cellular responses to MEI-1 treatment in wild type p53 and p53 null cancer cell lines.*

Leukemia and colorectal cancer cell lines were treated with MEI-1. MDM2/MDMX protein levels, p53-dependent and -independent cellular responses were examined following MEI-1 treatment by immunoblotting.

***Aim 4**. Assessment of the physical interaction between MEI-1 and the MDM2: MDMX RING domain heterodimer.*

The biochemical interaction between MEI-1 and recombinant MDM2: MDMX RING domain heterodimer was evaluated using Biolayer Interferometry technology to determine if MEI-1 was capable of binding to the MDM2: MDMX RING heterodimer.

In summary, this project aimed to investigate the inhibition of MDM2 by small molecule MEI-1 in various cancer cell lines to better evaluate the anti-cancer potential of MEI-1 as an MDM2 inhibitor. In addition, the mechanism of MDM2 inhibition by MEI-1 through its interaction with the MDM2: MDMX RING domain heterodimer was investigated.

Chapter 2: Materials and Methods

2.1. Cell Culture

The cell lines used in this study were grown in the respective media supplemented with 10% Fetal Bovine Serum (FBS) (Gibco, Cat. 12483-020) (Table 1). Specifically, adherent breast carcinoma MCF-7 cells and BJ-FB normal fibroblast cells were grown in DMEM medium supplemented with 10% FBS. p53 wild type leukemia AML-2 suspension cells were grown in MEM Alpha (1X) Minimum Essential medium containing 10% FBS. p53 null leukemia HL-60 suspension cells were grown in RPMI Medium 1640 (1X) with 10% FBS. Colorectal HCT-116 adherent cancer cells were grown in McCoy's 5A Medium (1X) Modified supplemented with 10% FBS. All cells were incubated at 37°C and with 5% CO_2.

Table 1: The cell lines used in this study and associated cell culture conditions

Cell Line	Type	P53 Status	Medium (supplemented with 10% FBS)
MCF-7	Breast Carcinoma (Adherent)	WT	DMEM (Gibco, Cat. 11995-065)
AML-2	Leukemia (Suspension)	WT	MEM Alpha (1X) Minimum Essential Medium (Gibco, Cat. 12571-063)
HL-60	Leukemia (Suspension)	Null	RPMI Medium 1640 (1X) (Gibco, Cat. 11875-093)
HCT-116 +/+	Colorectal Carcinoma (Adherent)	WT	McCoy's 5A Medium (1X) Modified (Gibco, Cat. 16600-082)
HCT-116 -/-	Colorectal Carcinoma (Adherent)	Null	McCoy's 5A Medium (1X) Modified (Gibco, Cat. 16600-082)
BJ-FB	Normal Fibroblast (Adherent)	WT	DMEM (Gibco, Cat. 11995-065)

2.2. MEI-1 Treatment Conditions

MEI-1 (Hinokiflavone) was purchased from *AvaChem Scientific*, diluted to 10 mM with DMSO (Sigma, D-8130) as a stock solution and stored in -80°C. MEI-1 was further diluted to specific concentrations as shown in Table 2 based on the cell lines and experimental assays conducted. For the cells treated with MEI-1, MEI-1 was diluted to final concentrations using cell specific media. Treated cells were incubated with MEI-1 and harvested after 24 hours.

Table 2: MEI-1 treatment conditions in different experiments

MEI-1 Concentration Range (µM)				
Cell Line	**Cell Viability Assay**	**Ubiquitination Assay**	**Immunoblot Analysis**	**Cellular Proliferation Assay**
MCF-7	0-50 µM	-	-	-
AML-2	0-25 µM	0-8 µM	0-8 µM	-
HL-60	0-25 µM	0-25 µM	0-8 µM	-
HCT-116 p53 WT	0-100 µM	-	0 - 50 µM	0 µM, 12 µM
HCT-116 p53 null	0-100 µM	-	0 - 50 µM	0 µM, 12 µM
BJ-FB	0-50 µM	-	-	-

2.3. Cell Viability Assay

Cell viability assay was performed using the *Celltiter Glo 2.0* kit (Promega, Cat. G9242) as per the manufactures' instructions. MEI-1 was added to cells (approximately 600,000 – 1.2 million cells) at various concentrations for 24 hours as described in Table 2. 100 µl of *Celltiter Glo 2.0* reagent was mixed with 100 µl of cell suspension. Cell viability luminescence was quantified with the Synergy Hybrid 4 reader. The IC_{50} value of MEI-1 on various cell lines was calculated with an online tool based off the equation $y = Min. + \frac{Max. - Min}{1 + (\frac{x}{IC50})^{Hill\ Coefficient}}$ (https://www.aatbio.com/tools/ic50-calculator). Standard deviation and standard error were

calculated based on experimental triplicates. Statistical analysis was performed through the pairwise Student T-test (* represents p-values < 0.05, ** represents p-values < 0.01, *** represents p-values < 0.001).

2.4. Ubiquitination Assay

AML-2 and HL-60 cells were incubated with a range of MEI-1 concentrations, as shown in Table 2, for 24 hours. The stock MG132 proteasome inhibitor (EMD Millipore, Cat. 474787-10mg) (20 mM) was diluted to a working concentration of 10 μM and added to cells for an additional 4 hours post MEI-1 treatment. Cells were harvested and lysed using RIPA buffer (50mM Tris buffer pH 8.0, 150mM NaCl, 0.5% NP 40) with additional 1×protease inhibitor (Complete, Cat. 05056489001, EDTA-free, Roche) and 20mM N- Ethylmaleimide (NEM) to inhibit proteases and deubiquitinating enzymes (Sigma, Cat. E3876). Total protein lysate (approximately 50 μg – 100 μg) was used for immunoblot analysis and resolved with 7.5% SDS-PAGE. Proteins were transferred to PVDF membranes (AmershanHybond, 0.2μm, Cat.10600021) for immunoblot detection of ubiquitinated MDM2 and p53 using respective antibodies (Table 3). Membranes were treated with Enhanced Chemiluminescence Substrate ECL (PerkinElmer, 203-17491) and imaged (Imager: MicroChemi Bio-Imaging Systems Cat. 70-25-00).

2.5. Immunoblot Analysis

Approximately 10^7 cells treated with MEI-1 were harvested after 24 hours and lysed with 1 mL of RIPA buffer (50mM Tris buffer pH 8.0, 150mM NaCl, 0.5% NP 40), 20 μL of 50X protease inhibitor (Complete, Cat. 05056489001, EDTA-free, Roche), 2 μL of fresh 1000X PMSF (1 mM) (Bioshop, PMS123), and 1 μL of Benzamidine (1mM) (Bioshop, BEN601).

Following the manufacture's protocol, a BCA assay (Pierce BCA Protein Assay Kit, Cat. 23225) was conducted to determine the protein concentration of each lysate. Protein lysates (50-100 μg of total protein) were mixed with 4X SDS-PAGE sample buffer and boiled at 95°C in SDS sample buffer for 5 minutes. Prepared samples were resolved on either 12% or 7.5% SDS-PAGE gels and immunoblotting was performed using respective primary antibodies found in Table 3. HRP-conjugated secondary antibodies, anti-rabbit (Jackson ImmunoResearch 711-035-152) and anti-mouse (Jackson ImmunoResearch 711-035-150), were diluted 1:5000 with 5% milk in TBST (1x PBS with addition of 0.1% Tween-20) and incubated with membranes for an additional hour. Membranes were treated with Enhanced Chemiluminescence Substrate ECL (PerkinElmer, 203-17491) and imaged (Imager: MicroChemi Bio-Imaging Systems Cat. 70-25-00).

2.6. Antibodies

The primary antibodies used in this study include mouse monoclonal against MDM2 (Santa Cruz, sc-965), MDMX (Millipore 8C6, 04-1555), p53 (Santa Cruz DO-1, sc-126), Rb (Cell Signaling #9307), GAPDH (Cell Signaling #2118), rabbit monoclonal against phosphorylated p53 (serine 15) (Cell Signaling, #9284P), and rabbit polyclonal against PARP (Cell Signaling #9542), cleaved Caspase-9 (Cell Signaling #9505), and Foxo3a (Cell Signaling, #2497) (Table 3.) HRP-conjugated secondary antibodies used in immunoblot analysis were anti-rabbit (Jackson ImmunoResearch 711-035-152) and anti-mouse (Jackson ImmunoResearch 711-035-150).

Table 3: Primary antibodies used for immunoblotting analysis

Primary Antibody	Molecular Weight (kDa)	Species	Company, Catalogue #	Dilution Factor using TBST
MDM2	90	Mouse monoclonal	Santa Cruz, sc-965	1:1000 in 5% BSA
MDMX, clone 8C6	80	Mouse monoclonal	Millipore, 04-1555	1:1000 in 5% BSA
p53 (DO-1)	53	Mouse monoclonal	Santa Cruz, sc-126	1:1000 in 5% milk
Phosphorylated p53 (ser 15)	53	Rabbit monoclonal	Cell Signaling #9284P	1:1000 in 5% milk
PARP	116 (full length) 89(cleaved)	Rabbit polyclonal	Cell Signaling, #9542	1:1000 in 5% milk
Cleaved Caspase-9	35	Rabbit polyclonal	Cell Signaling, #9505	1:1000 in 5% milk
Rb	110	Mouse monoclonal	Cell Signaling #9307	1:200 in 5% milk
Foxo3a	82	Rabbit polyclonal	Cell Signaling, #2497	1:1000 in 5% BSA
GAPDH	36	Mouse monoclonal	Cell Signaling #2118	1:200 in 5% milk

2.7. Cell Proliferation Assay

HCT-116 p53 wild type and p53 null cells were counted with a hemocytometer and diluted to 100,000 cells, which were incubated with MEI-1 (0 μM or 12 μM) and grown for six days. The cells were replenished with fresh media and MEI-1 every two days. The cells were counted and monitored every 24 hours for six days.

2.8. MDM2 and MDMX RING Domain Protein Expression and Purification

His-tagged MDMX RING domain (residues 416-490) was cloned in pET15b plasmid and GST-tagged MDM2 RING domain (residues 417-491) was cloned in pGEX2TK plasmid. Both were expressed in *E.coli BL21 DE3* cells at 18°C using LB broth and induced using 0.5 mM IPTG (Isopropyl β- d-1-thiogalactopyranoside). Purification of the recombinant MDM2: MDMX RING heterodimer was conducted through sequential affinity chromatography using GST- affinity chromatography, followed by

Ni^{2+} affinity chromatography purification. Briefly, the GST-tagged MDM2 RING domain and His-tagged MDMX RING domain cells were mixed and lysed in lysis buffer (50 mM Tris pH 7.5, 500 mM NaCl, 10% glycerol, 50 uM $ZnCl_2$, 0.5 mM PMSF, 10 mM β-mercaptoethanol, 0.1% Triton-X). The lysate was cleared by centrifugation and incubated with the GST resin for 1 hour. The immobilized protein was washed with wash buffer (50 mM Tris pH 7.5, 500 mM NaCl, 10% glycerol, 50 uM $ZnCl_2$, 0.5 PMSF, 10 mM β-mercaptoethanol). Proteins were eluted in a buffer containing 50 mM Tris, 30 mM reduced glutathione, 500 mM NaCl, 10% glycerol, 50 uM $ZnCl_2$, 10 mM β-mercaptoethanol in pH 7.5. The eluate from GST purification was loaded to a Ni^{2+} column and incubated for 30 minutes. The immobilized protein was washed extensively with a buffer (50 mM Tris pH 7.5, 500 mM NaCl, 10% glycerol, 50 uM $ZnCl_2$, 1 mM benzamidine, 0.5 mM PMSF, 1 mM β-mercaptoethanol, and 20 mM imidazole), then eluted with the elution buffer (50 mM Tris pH 7.5, 500 mM NaCl, 10% glycerol, 50 uM $ZnCl_2$, 1 mM benzamidine, 0.5 mM PMSF, 1 mM β-mercaptoethanol, 500 mM imidazole). Samples were taken from each step of sequential purification and resolved on SDS-PAGE gel. The purified MDM2: MDMX RING heterodimer was dialyzed with 50 mM Tris pH 7.5, 150 mM NaCl, and 10% glycerol prior to BLI analysis.

2.9. Biolayer Interferometry (BLI) Assay

BLI analysis was performed using the BLI Octet Red from fortéBIO. MEI-1 was diluted to the final concentrations ranging from 0 μM to 126 μM using an assay buffer (20 mM MOPS (3-(N-Morpholino) propane sulfonic acid), Tris (Tris(hydroxymethyl)amino-methane) (added to adjust pH to 8.0), 50 mM KCl, BSA fatty-acid free, 0.5 mg/ml final). A sensory probe (Anti-GST Biosensor 18-5095 fortéBIO) coated with GST antibody was loaded with GST-tagged MDM2: His-tagged MDMX RING heterodimer (100 μL of 2 mg/mL). GST alone was loaded

onto the anti-GST biosensor probe and served as the negative control. To quantify the protein association and the dissociation between MEI-1 and the MDM2: MDMX heterodimer interaction, the biosensor was incubated with different concentrations of MEI-1 (0 μM – 126 μM) for 400 seconds. The BLI signal was recorded for a total of 3000 seconds. Data fitting and kD calculation were determined through data analysis v9.0 software (fortéBIO, Pall Corp., USA) using one binding site model. Similar experiment was conducted using a His biosensor probe (Anti-Penta-HIS Biosensor 18-5077 fortéBIO) with the same experimental conditions.

Chapter 3: Results

(I would like to thank Ernest Tsang and Milena Gatto for contributing to some experiments as part of their undergraduate training as well as Dr. Yi Sheng for helping with the BLI octet assay.)

3.1. MEI-1 Decreases Cell Viability in AML-2 and HL-60 Leukemia Cells

AML-2 and HL-60 are both leukemia cancer cell lines with MDM2 overexpression (Bueso-Ramos et al., 1993). AML-2 encodes a wild type *TP53* gene whereas HL-60 has a *TP53* gene deletion. To reveal whether the p53 status and MDM2 expression levels affects cellular responses to MDM2 inhibition by MEI-1, AML-2 and HL-60 cell lines were selected for this study.

To evaluate the effect of MEI-1 on AML-2 and HL-60 leukemia cells, the *Celltiter-Glo 2.0* assay was used to measure cell viability following MEI-1 treatment. This assay quantifies the number of metabolically active cells and generates a luminescent signal proportional to the amount of ATP present in the cell, which is directly proportional to the number of live cells present in culture (Figure 3.1A-B) (Hannah et al., 2001). In order to assess cell viability, the cell lines were treated with MEI-1 at a range of concentrations (0-25 μM) for 24 hours, in triplicates (Figure 3.1B).

As shown in Figure 3.1C, MEI-1 treatment decreased cell viability in both AML-2 and HL-60 leukemia cells. Results indicated that cell viability dramatically decreased as the concentration of MEI-1 increased (Figure 3.1C). The IC_{50} value of MEI-1 in AML-2 cells was 4.39 ± 1.16 μM. HL-60 cells were found to be less sensitive to MEI-1 treatment, with an IC_{50} value of 10.95 ± 0.19 μM (Figure 3.1C). Statistical analysis (pairwise Student T-test) showed a significant difference in cell viability between MEI-1 treated AML-2 cells and HL-60 cells at all tested MEI-1 concentrations ranging from 3 μM to 25 μM, further confirming that MEI-1 induced more cell death in AML-2 than in HL-60 cells (Figure 3.1C). Overall these results suggest that MEI-1 induced cytotoxicity in both leukemia cell lines. As the AML-2 cancer cells contained the wild type *TP53* gene and demonstrated better sensitivity to MEI-1 treatment than

p53 null HL-60 cells, this suggested that the effect of MEI-1 could be p53-dependent. However, as HL-60, the p53 null cell line, was also shown to be affected by MEI-1 treatment, this revealed that MEI-1 exerted additional p53 independent cytotoxicity.

A)

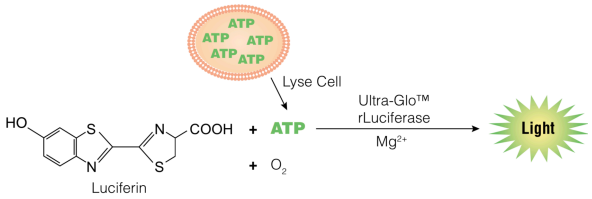

B)

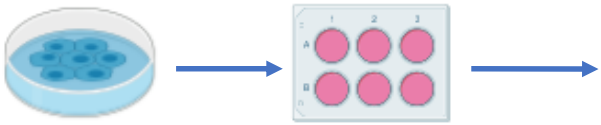

Cell Viability assay using
CellTiter Glo 2.0

MEI-1 treatment at various
concentrations for 24h

C)

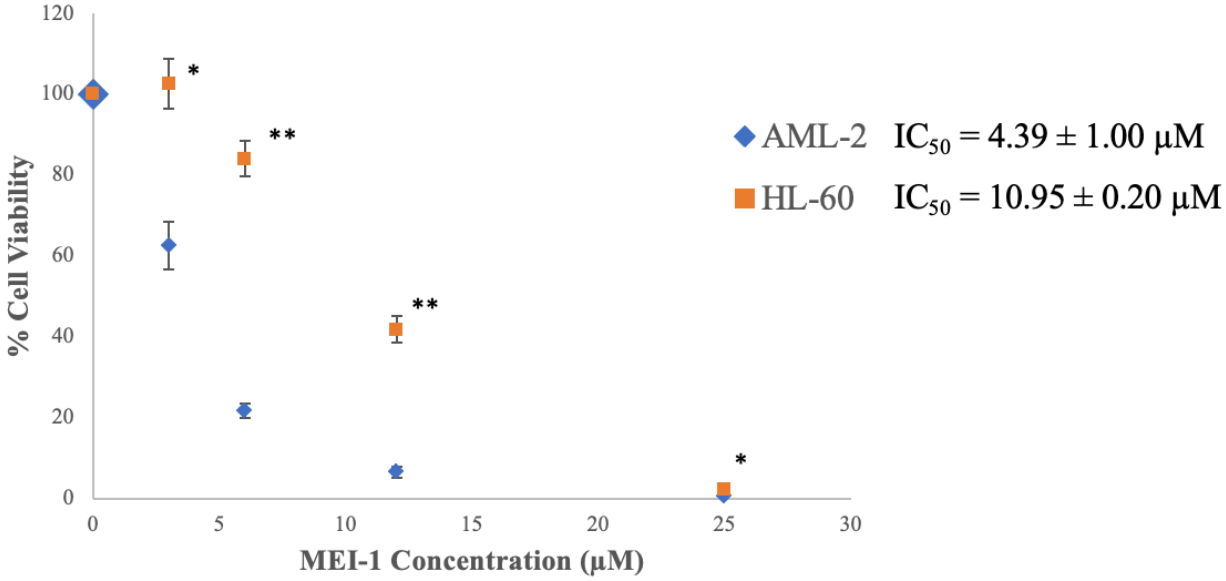

Figure 3.1 (A-C). MEI-1 affects cell viability of AML-2 and HL-60 cells. (A) Cell viability was evaluated using *CellTiter-Glo 2.0* reagent based on cellular ATP production. The figure is taken from *Promega CellTiter-Glo 2.0 assay protocol.* (B) Schematic depiction of MEI-1 treatment in cell viability assay. The image is created with Biorender.com (C) Comparison of cell viability of AML-2 and HL-60 cells following MEI-1 treatment. Three trials were conducted (N=3). Results were presented as percentage of viability and normalized against initial cell number. The IC_{50} values (µM) are represented by Mean ± SEM (± 0.20 – 1.00 µM). SD values of both cell lines rounded to 2 decimal places for each concentration of MEI-1 (0-25 µM). Statistical analysis were performed between AML-2 and HL-60 cells for each MEI-1 concentration using pairwise student t-test. (*) p-values < 0.05, (**) p-values < 0.01.

3.2. MEI-1 inhibits MDM2-Mediated Ubiquitination in AML-2 and HL-60 Leukemia Cells

MEI-1 was identified as a small molecule from an *in silico* screening shown to interact with the MDM2 RING domain and hypothesized to block E3 ligase activity of MDM2. *In vitro* ubiquitination assays were previously conducted to show that MEI-1 blocks MDM2 mediated auto- and p53 ubiquitination using recombinant E1, E2 and MDM2 (unpublished, Sheng lab). Therefore, further tests on whether MEI-1 inhibits MDM2-mediated ubiquitination in AML-2 and HL-60 cells were performed.

AML-2 cells were treated with MEI-1 in a range of concentrations between 0 and 8 μM for 24 hours. Proteasome inhibitor MG132 (10 μM) was added for 4 hours following MEI-1 treatment to enrich ubiquitinated MDM2 and p53 proteins in cells. Cells were lysed with N-ethylmaleimide (NEM, 20 mM) to inhibit the activities of deubiquitinating enzymes. Ubiquitinated MDM2 and p53 were detected by immunoblotting and observed as high molecular weight protein smears when cells were treated with MG132 (Figures 3.2-3.3). Decreased ubiquitinated MDM2 and p53 levels were observed when cells were treated with 8 μM MEI-1 and MG132 (Figures 3.2A-B). AML-2 cells were also tested with a wider range of MEI-1 (0 – 25 μM) and results confirmed that inhibition appeared at greater concentrations (Figure 3.2C). Statistical analysis (pairwise Student T-test) showed a significant difference between increasing concentrations of MEI-1 treated AML-2 cells (0.5 - 8 μM, 1.5 - 25 μM) and non-treated AML-2 cells, with the presence of MG132, indicating that ubiquitination was affected with greater concentrations of MEI-1 (Figure 3.2 A-C). Hence, MEI-1 could attenuate MDM2 and p53 ubiquitination in AML-2 cells, which was consistent with the observation made from *in vitro* ubiquitination assay, supporting the role of MEI-1 as an inhibitor of MDM2 E3 ligase.

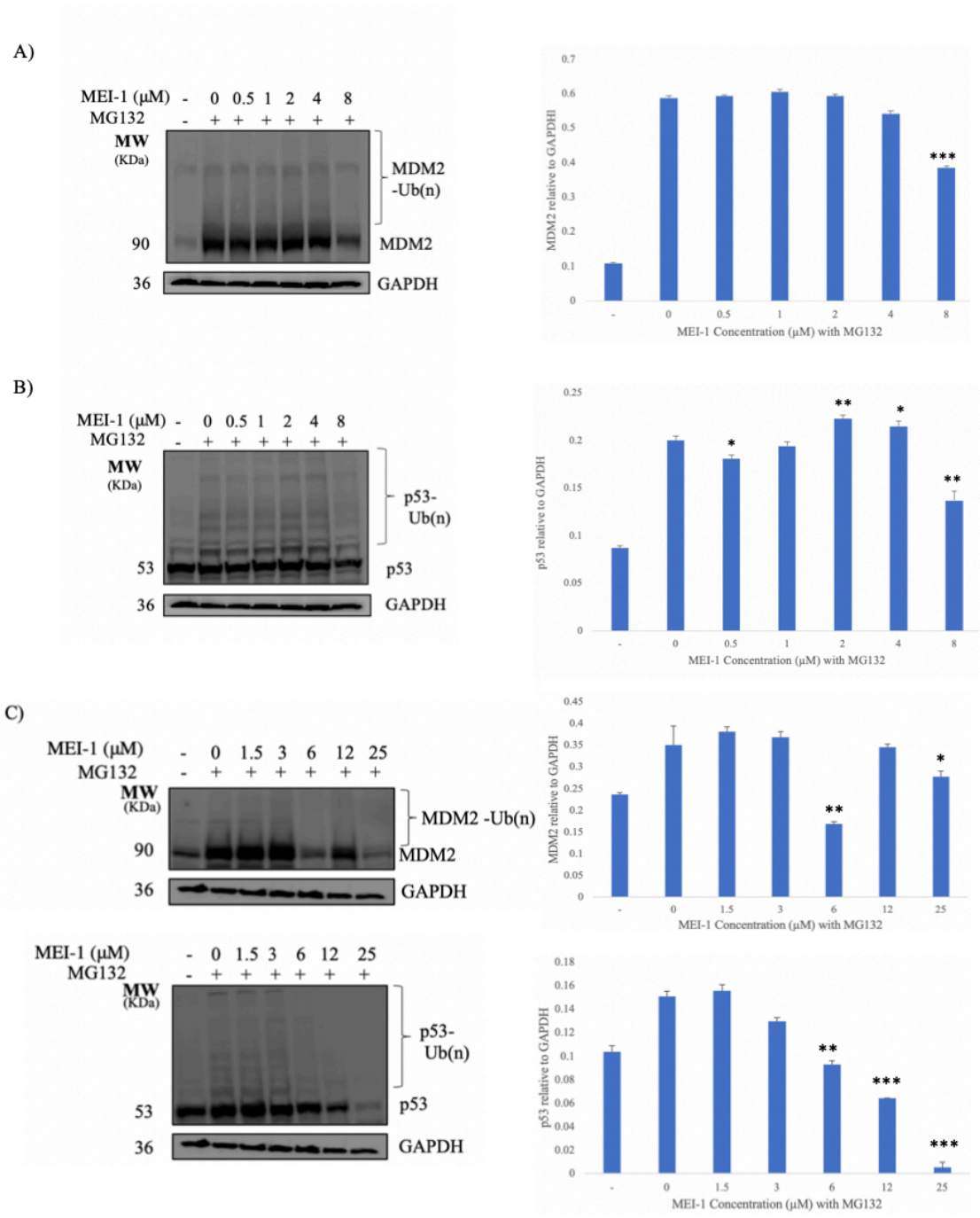

Figure 3.2 (A-C). MEI-1 attenuates MDM2 and p53 ubiquitination in AML-2 cells. AML-2 cells were treated with a range of MEI-1 concentrations (0 – 8 μM, 0-25 μM) for 24 hours followed by a 4-hour treatment with proteasome inhibitor MG 132 (10 μM). Immunoblotting was used to detect polyubiquitinated MDM2 (A, C) and p53 (B, C) levels in response to MEI-1 treatment. Statistical analysis was performed between each MEI-1 concentration (0.5 – 8 μM, 1.5 – 25 μM) against no treatment using pairwise student t-test. (*) p-values < 0.05, (**) p-values < 0.01, (***) p-values < 0.001. GAPDH was used as a loading control. Three trials were conducted (N=3). Protein levels were quantified using densitometry on ImageJ.

A cellular ubiquitination assay was also performed in the p53 null HL-60 leukemia cell line. Different from AML-2 treated cells, HL-60 cells were treated with a range of 0-25 μM of MEI-1 for 24 hours, followed by the addition of MG132 (10 μM) for 4 hours. Similar to what was observed in AML-2 cells, HL-60 cells treated with MEI-1 with concentrations of 12 μM and higher resulted in decreased levels of MDM2 ubiquitination (Figure 3.3).Statistical analysis (pairwise Student T-test) showed a significant difference in HL-60 treated cells with MG132, from the lowest concentration of MEI-1 (1.5 μM) and onwards, as compared to HL-60 non-treated cells with MG132 (Figure 3.3). This result agreed with what was shown with AML-2 cells, suggesting that MEI-1 as a potential MDM2 antagonizer could effectively inhibit MDM2 mediated-ubiquitination in HL-60 cells.

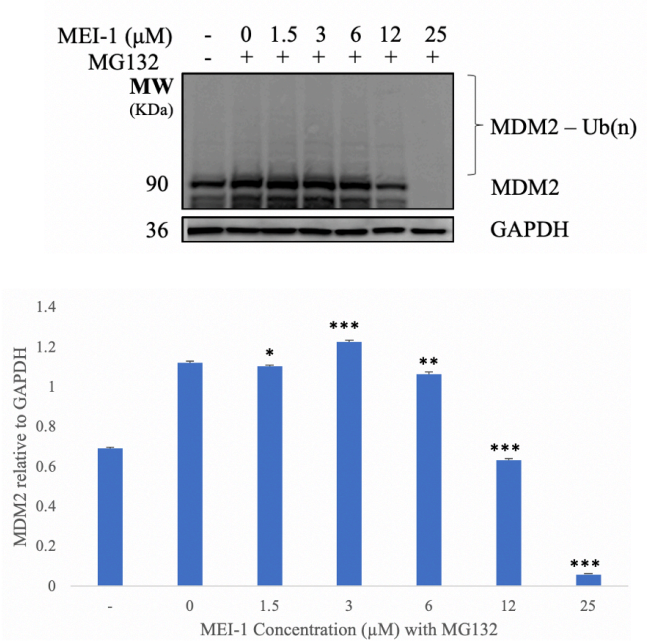

Figure 3.3 MEI-1 inhibits MDM2 ubiquitination in HL-60 cells. HL-60 cells were treated with a range of MEI-1 concentrations (0 – 25 μM) for 24 hours followed by a 4-hour treatment with proteasome inhibitor MG 132 (10 μM). Immunoblotting was used to detect polyubiquitinated MDM2 levels in response to MEI-1 treatment.Statistical analysis was performed between each MEI-1 concentration (1.5 – 25 μM) against no treatment using pairwise student t-test. (*) p-values < 0.05, (**) p-values < 0.01, (***) p-values < 0.001. GAPDH was used as loading control. Three trials were conducted (N=3). Protein levels were quantified using densitometry on ImageJ.

3.3. Cellular Responses to MEI-1 treatment in AML-2 and HL-60 Cells

The MDM2: MDMX heterodimer is the primary form of the MDM2 E3 ligase in the cell. It has been shown that MDMX and p53 are directly targeted by MDM2 for ubiquitination and proteasomal degradation (Chen & Pan, 2003; Linares et al., 2003). Therefore, inhibition of MDM2/MDMX E3 ligase activity by MEI-1 is expected to prevent MDM2 mediated auto-ubiquitination and ubiquitination of MDMX and p53. In addition, MDM2 also serves as a ubiquitin E3 ligase for two cellular regulatory proteins, Rb and Foxo3a, and has been shown to regulate their stability in the cell. The effect of MEI-1 was examined on the steady levels of these proteins through western blot analysis.

AML-2 and HL-60 cell lines were treated with a range of MEI-1 concentrations (0 - 8 μM) for 24 hours, respectively. The effect of MEI-1 treatment in AML-2 cells is shown in Figure 3.4A. The levels of MDM2 and MDMX exhibited a bimodule effect upon the addition of MEI-1. An increase of MDM2/MDMX protein levels was observed at lower doses (0.5 – 2 μM) of MEI-1. However, the levels of MDM2/MDMX were shown to decrease at higher doses (4 - 8 μM), while increased cell death (>50% cell death) was observed under the same doses of MEI-1 treatment (Figure 3.4A).

HL-60 cells were treated with the same range concentrations of MEI-1. Similar to AML-2 results, HL-60 cells also exhibited a bimodule effect on MDM2 and MDMX protein levels. MDM2/MDMX levels increased at lower concentrations of MEI-1 (0.5 – 2 μM) and decreased at higher concentrations (4 – 8 μM) (Figure 3.4B). Based on these results, MEI-1 appears to inhibit MDM2/MDMX E3 ligase activity at a range of 0.5 - 2 μM, supporting MEI-1's role as a potential inhibitor of MDM2/MDMX at these concentrations. Under higher concentrations of

MEI-1 treatment, MEI-1 induced the de-stabilization of MDM2/MDMX, which seems to coincide with increased cell death in these cells.

The leukemia cell lines with wild type p53 were shown to be sensitive to p53 activation and p53-dependent apoptosis. To elucidate the effect of MEI-1 on p53 stability and activity through MDM2/MDMX inhibition, AML-2 and HL-60 cancer cells were treated with MEI-1 under similar conditions as described above and the levels of total p53 and the transcriptionally active form of p53 (phosphorylated p53 at serine 15) were examined.

As shown in Figure 3.4A, MEI-1 appeared to activate p53 in AML-2 leukemia cells. Total p53 levels steadily increased and plateaued upon MEI-1 treatment (Figure 3.4A). The levels of phosphorylated p53 increased from 4 μM and onwards (Figure 3.4A). These results suggest that p53 could be stabilized by MEI-1, likely through the inhibition of MDM2/MDMX. p53 activation was observed at higher doses of MEI-1 treatment, opposing to the decreasing trend of MDM2/MDMX levels under these concentrations. Agreeing with the p53 null status of HL-60 cells, p53 and phosphorylated p53 were not detected (Figure 3.4B).

Western blot analysis was performed to examine cleaved PARP (Poly ADP-ribose polymerase) and cleaved caspase-9, which serve as cell apoptotic markers. Procaspase-9 is 47 kDa in size. Upon apoptotic stimulation, procaspase-9 is cleaved into its active form, the 35 kDa caspase-9. In this study, only cleaved caspase-9 (35 kDa) was examined and shown. Full length PARP is 116 kDa. In early apoptosis, PARP is cleaved by the executioner caspase-3 to be 89 kDa in size. As shown in Figure 3.4A, AML-2 cells exhibited a low level of cleaved caspase-9 in the absence of MEI-1. A steady increase of cleaved caspase-9 was shown upon MEI-1 treatment, with greater accumulation at doses of 4 – 8 μM (Figure 3.4A). Similarly, PARP cleavage steadily

increased, while full length PARP decreased in AML-2 cells upon the MEI-1 treatment (Figure 3.4A). PARP cleavage was most noticeable at higher doses of MEI-1 treatment, 4 μM and onwards (4 - 8 μM). These results suggest that increased cell death may be a result of apoptosis upon treatment of MEI-1 in AML-2 cells. HL-60 cells exhibited a similar apoptotic response upon MEI-1 treatment, with cleaved PARP and cleaved caspase-9 observed from 4 μM and higher of MEI-1 (Figure 3.4B). These results suggest that the HL-60 cells have also undergone apoptosis with treatment of MEI-1.

Lastly, tumour suppressors Rb and Foxo3a have both been shown to be directly affected by MDM2 E3 ligase activity. In order to determine whether MEI-1 treatment induced p53-independent cellular responses, the effect of MEI-1 on Rb and Foxo3a protein levels was examined. MEI-1 treatment resulted in the steady accumulation of Rb in both AML-2 and HL-60 cells, peaking at 2 μM (Figure 3.4), suggesting that MEI-1 could stabilize Rb through the inhibition of MDM2/MDMX activity. Interestingly, the levels of Foxo3a exhibited a different pattern upon MEI-1 treatment in AML-2 and HL-60 cells. At lower concentrations (0 – 2 μM) of MEI-1 treatment, a stabilization of Foxo3a levels was observed in AML-2 cells, whereas Foxo3a levels were shown to decrease at higher concentrations (4 - 8 μM) (Figure 3.4A). This result was similar to the bimodule effect of MEI-1 previously observed in MDM2/MDMX. On the other hand, MEI-1 treatment of HL-60 cells exhibited a steady accumulation of Foxo3a, following a similar trend observed in Rb (Figure 3.4B), despite low signal intensity of Foxo3a in HL-60 cells. Taken together, Rb and Foxo3a levels were affected by MEI-1 treatment. Whether the effect resulted from inhibition of Rb and Foxo3a ubiquitination by MEI-1 requires further investigation.

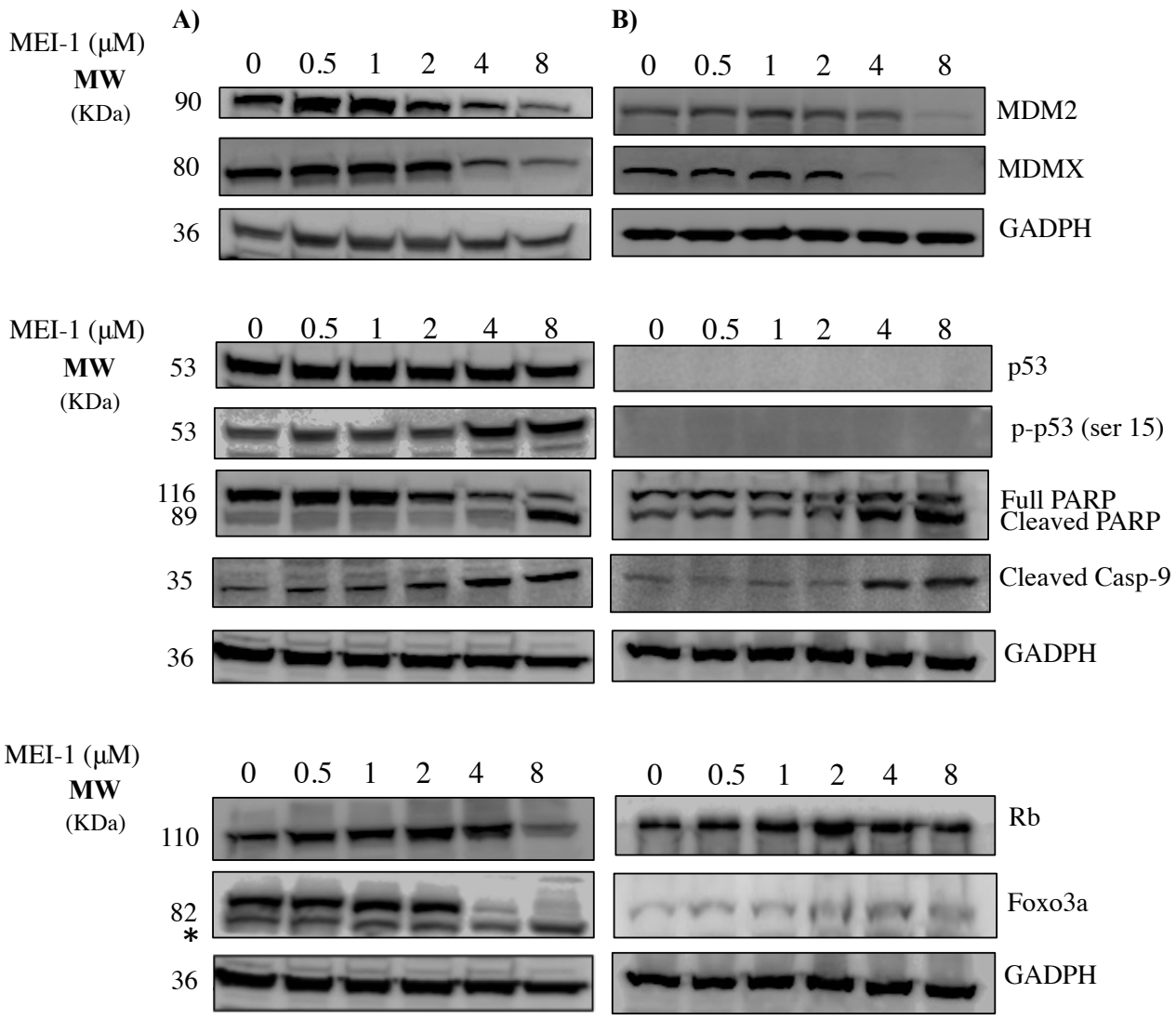

Figure 3.4 (A-B). Immunoblot analysis of AML-2 and HL-60 cells with MEI-1 treatment. (A) AML-2 and (B) HL-60 cells were treated with a range of MEI-1 concentrations (0 - 8 μM) for 24 hours followed by immunoblotting for: MDM2, MDMX, p53, phosphorylated p53 at Ser 15, Rb, Foxo3a, cleaved PARP and cleaved caspase-9. GAPDH was used as a loading control. 100 micrograms of total cell lysate was used for each lane. Asterisk (*) represents protein degradation.

3.4. MEI-1 Decreases Cell Viability in HCT-116 p53 WT and HCT-116 p53 Null Colorectal Cancer Cells

Two colorectal cancer cell lines were selected to further explore the p53-dependent and p53-independent effects of MEI-1 in cells. HCT-116 p53 WT features a wild type *TP53* gene whereas HCT-116 p53 null has *TP53* gene knocked out. Unlike the AML-2 and HL-60 leukemia cell lines, these two HCT-116 cell lines have a similar genetic background, and therefore were specifically selected to reveal whether p53 status could affect the cellular responses to MEI-1 treatment.

The *Celltiter-Glo 2.0* assay was used to measure cell viability of HCT-116 p53 WT and HCT-116 p53 null cells in response to MEI-1 treatment. When HCT-116 p53 WT and HCT-116 p53 null cells were treated with MEI-1 at a range of concentrations (0-100 μM) for 24 hours, both cell lines showed decreased cell viability but appeared to be less sensitive to MEI-1 treatment when compared to leukemia AML-2 and HL-60 cells (Figure 3.5B vs. Figure 3.1C). As the concentration of MEI-1 increased from 0-100 μM, cell viability decreased to 7% in HCT-116 p53 WT cells and 13% in HCT-116 p53 null cells, respectively. (Figure 3.5B). The cell viability assay revealed that MEI-1 had a significant cytotoxic effect on both HCT-116 p53 WT and HCT-116 p53 null cell lines. Furthermore, HCT-116 p53 WT treated cells were more sensitive to MEI-1 treatment than HCT-116 p53 null treated cells. Statistical analysis (pairwise Student T-test) showed a significant difference (p-value < 0.001) between the two cell types, indicating HCT-116 p53 WT cells were significantly more sensitive than HCT-116 p53 null cells to MEI-1 treatment (Figure 3.5B). The IC_{50} values for HCT-116 p53 WT and HCT-116 p53 null cells were 14.19 ± 2.04 and 32.66 ± 0.31, respectively (Figure 3.5B). The fact that MEI-1 showed an increased inhibitory potency in HCT-116 p53 WT cells compared to HCT-116 p53 null cells suggests that MEI-1 played a role in the p53-dependent pathway. However, MEI-1 also

exhibited cytotoxicity in HCT-116 p53 null cells, suggesting that MEI-1 partook in p53-independent pathways, similar to previously discussed HL-60 treated cells.

A)

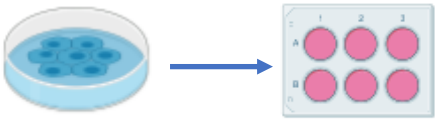

Cell Viability assay using *CellTiter Glo* 2.0

MEI-1 treatment at various concentrations for 24h

B)

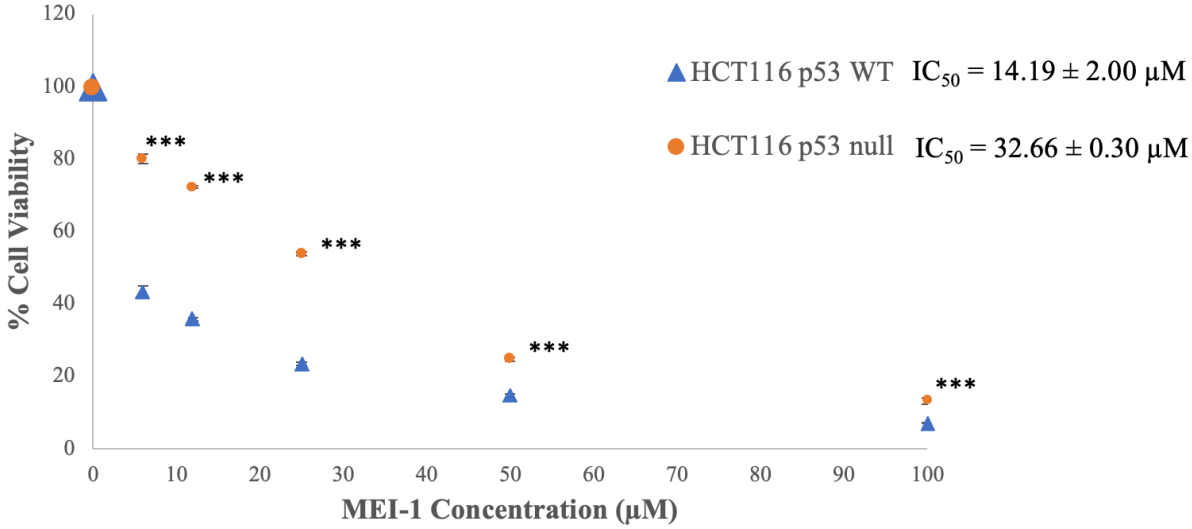

Figure 3.5 (A-B). The effect of MEI-1 on cell viability in HCT-116 p53 WT and HCT-116 p53 null cells. (A) Schematic representation of MEI-1 treatment and cell viability assay. The image was created with Biorender.com. (B) HCT-116 p53 WT and HCT-116 p53 null cell viability under MEI-1 treatment. Three trials were conducted (N=3). Results were presented as percentage of viability and normalized against initial cell number. The IC_{50} values (µM) are represented by Mean ± SEM (± 0.30 – 2.00 µM). SD values of both cell lines rounded to 2 decimal places for each concentration of MEI-1 (0-100 µM). Statistical analysis (pairwise student t-test) graph representation between two groups. (***) represents p-values < 0.001.

3.5. The Effect of MEI-1 on HCT-116 p53 WT and HCT-116 p53 Null Cellular Responses

Similar to what was described previously in the leukemia cells, MEI-1 was tested in both colorectal cancer cell lines, HCT-116 p53 WT and HCT-116 p53 null, and immunoblotting was performed to better understand the effect of MEI-1 on p53-dependent and p53-independent cellular responses in these two genetically similar cell lines.

Both HCT-116 p53 WT and HCT-116 p53 null cells were treated with MEI-1, ranging from 0 μM - 50 μM, for 24 hours. As shown in Figure 3.6A, MEI-1 treatment in HCT-116 p53 WT cells resulted in a bimodule effect on the MDM2/MDMX protein levels. MDM2/MDMX levels appeared to be stable from 3 μM - 6 μM and degraded at higher concentrations of MEI-1 (25 - 50 μM) (Figure 3.6A). These results agreed with what was observed in the AML-2 and HL-60 cells, supporting MEI-1 acting through inhibition of MDM2/MDMX E3 ligase and destabilization of the MDM2/MDMX heterodimer.

HCT-116 p53 null cells were treated under similar conditions. In contrast to HCT-116 p53 WT, MDM2/MDMX protein levels in HCT-116 p53 null cells remained stable at 3 μM and degraded at higher concentrations of MEI-1 (6 μM – 50 μM) (Figure 3.6B). Based on these results, MEI-1 appeared to destabilize MDM2/MDMX heterodimer, which is independent of p53 (Figures 3.6B, 3.4B).

Next, MEI-1's effect on p53 stability was examined in HCT-116 p53 WT cells. Total p53 protein levels and the transcriptionally active form of p53 (phosphorylated p53 at serine 15) were examined with immunoblot analysis. As depicted in Figure 3.6A, total p53 and the phosphorylated p53 levels appeared to be mildly increased in HCT-116 p53 WT cells at the

MEI-1 concentrations between 3 μM – 12 μM. When compared to previously tested AML-2 p53 WT cells, the signals for serine 15 phosphorylated p53 were weaker in HCT-116 p53 WT cells but the trend followed what was previously observed in AML-2 cells (Figures 3.4A, 3.6A). As expected for HCT-116 p53 null cells, the total levels of p53 and phosphorylated p53 were not observed (Figure 3.6B). These results in principle agreed with what was observed in AML-2 and HL-60 cells and implied that MEI-1 could stabilize and activate p53 through the inhibition of MDM2/MDMX.

The cleaved PARP and cleaved caspase-9 as cellular apoptotic markers were examined in the HCT-116 colorectal cancer cell lines. In both cell lines, cleaved PARP was seen with MEI-1 treatment using the concentrations of 12 μM or greater (12 μM – 50 μM) (Figures 3.6A-B). Cleaved caspase-9 was seen at low levels and became more prominent at 50 μM of MEI-1 treatment (Figures 3.6A-B). These results indicate there was induced apoptosis in HCT-116 p53 WT cells and HCT-116 p53 null cells upon MEI-1 treatment (Figures 3.5A-B).

Lastly, the effect of MEI-1 on two tumour suppressors, Rb and Foxo3a, were assessed in HCT-116 colorectal cancer cells. In HCT-116 p53 WT cells, upon the addition of MEI-1, there appeared to be a slight accumulation of Rb at the lower concentrations of MEI-1 (3 μM – 12 μM) and a decrease of Rb at the greatest concentration (50 μM) (Figure 3.6A). In HCT-116 p53 null cells, Rb did not appear to have a consistent response to MEI-1 treatment (Figure 3.6B). The levels of Rb were lower at MEI-1 concentrations between 3 μM and 12 μM , and gradually increased with higher concentrations of MEI-1 treatment (25 – 50 μM) (Figure 3.6B). Foxo3a levels were examined in HCT-116 p53 WT and p53 null cells. Foxo3a protein levels were found stabilized at lower concentrations of MEI-1 and degraded at higher concentrations of MEI-1 in

both cell lines (Figure 3.6B). Although Rb and Foxo3a levels appeared to be affected by MEI-1 treatment, more experiments will be required to elucidate whether MEI-1 has an effect on Rb and Foxo3a through inhibition of MDM2.

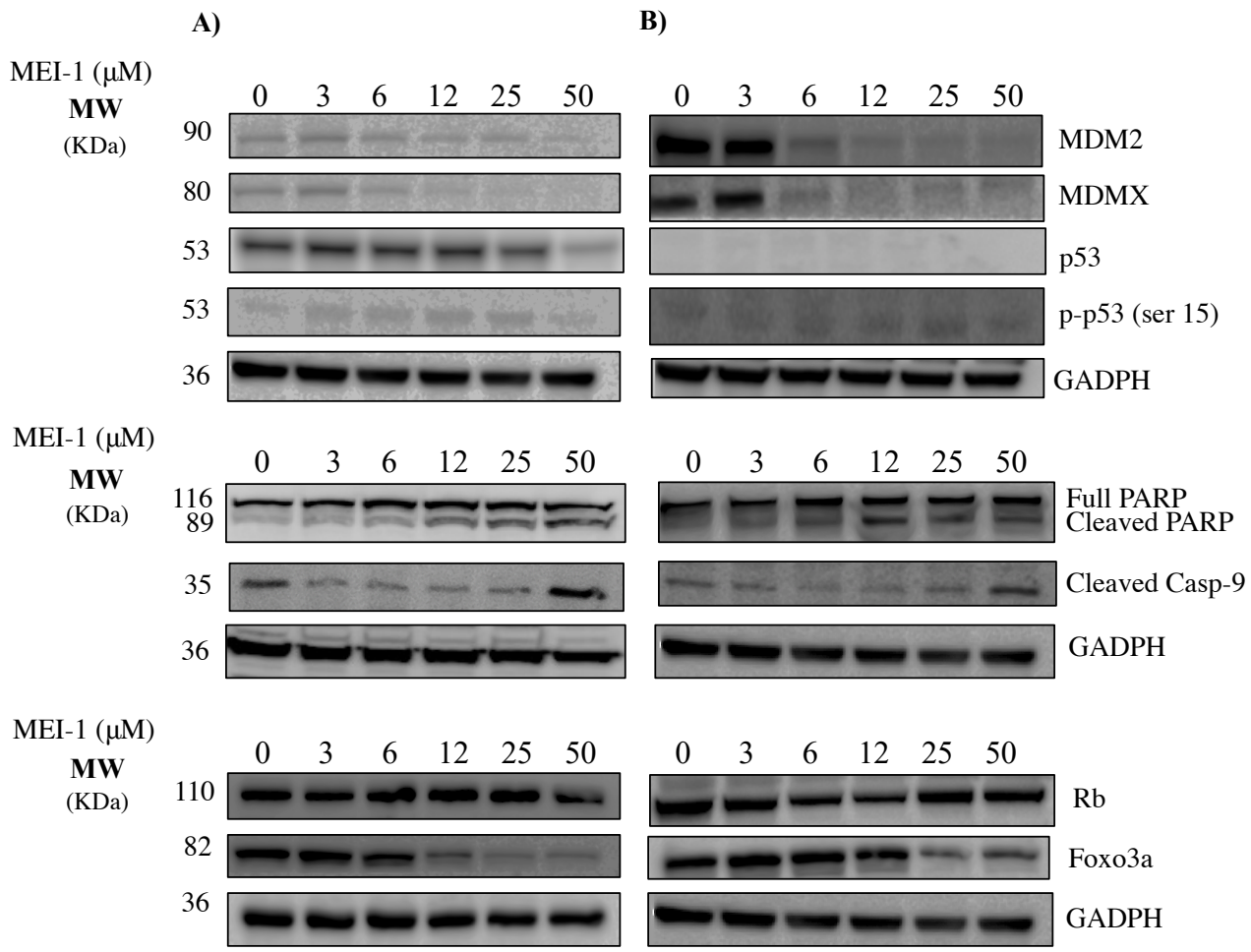

Figure 3.6 (A-B). Immunoblotting of HCT-116 p53 WT and HCT-116 p53 null cells with MEI-1 treatment. (A) HCT-116 p53 WT and (B) HCT-116 p53 null cells were treated with a range of MEI-1 concentrations (0 - 50 μM) for 24 hours followed by immunoblotting for MDM2, MDMX, p53, phosphorylated p53 at Ser 15, Rb, Foxo3a, cleaved PARP and cleaved caspase-9. GAPDH was used as a loading control.

3.6. MEI-1 Inhibits Cell Proliferation in HCT-116 p53 WT and p53 Null Cells

A proliferation assay was conducted in HCT-116 p53 WT and p53 null cells to determine the effect of MEI-1 on cell growth. In this experiment, cells were treated with 0 μM or 12 μM concentrations of MEI-1, respectively. The MEI-1 concentration of 12 μM chosen for cell treatment in this assay was close to the IC_{50} value of MEI-1 in HCT-116 p53 WT cells (Figure 3.5B). Cell growth was monitored for six days and cells were counted manually each day with a hemocytometer (Figure 3.7A).

As shown in Figure 3.7B, in the absence of MEI-1, both colorectal cancer lines exhibited a similar exponential growth over the course of six days (Figure 3.7B). MEI-1 treatment at 12 μM induced a continuous increase in cell death in both cell lines (Figure 3.7C-D). Compared to HCT-116 p53 null cells, HCT-116 p53 WT treated cells showed a slightly accelerated cell death (Figure 3.7C). These results showed that MEI-1 treatment inhibited cell proliferation in both colorectal cancer cell lines, and the p53 WT cells were more responsive to MEI-1 treatment, which was consistent with the previous findings of the cytotoxic effect of MEI-1 in these cells.

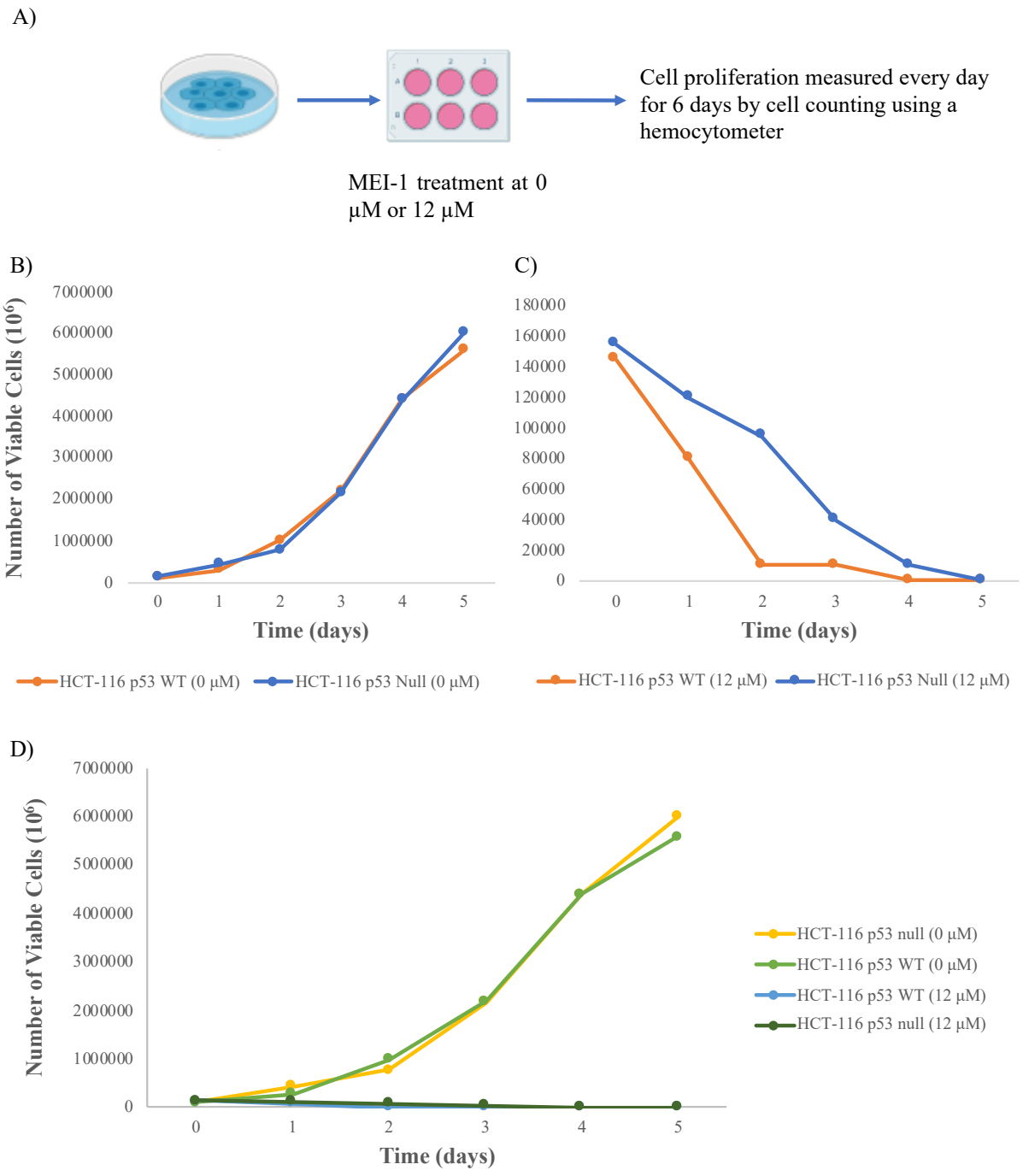

Figure 3.7 (A-D). The effect of MEI-1 on cell growth of HCT-116 p53 WT and HCT-116 p53 null cells. (A) Schematic diagram of MEI-1 treatment in a cell proliferation assay. The image was created with Biorender.com. (B-D) Cell growth was examined using a proliferation assay to determine the effect of MEI-1 on growth inhibition in colorectal cancer cell lines. Cells were treated with 0 µM or 12 µM of MEI-1, respectively, over a period of 6 days. Cells were counted manually with a hemocytometer.

3.7. The Cytotoxicity Effect of MEI-1 in Breast Carcinoma Cells and Normal Fibroblast Cells

To survey the cytotoxicity of MEI-1 in normal versus cancer cells, a normal fibroblast cell line, BJ-FB, and an adherent epithelial breast cancer line, MCF-7, were treated with MEI-1 and compared to AML-2, HL-60, and HCT-116 colorectal cancer cells.

MCF-7 and BJ-FB cells were treated with MEI-1 at a range of concentrations (0 - 50 μM) for 24 hours (Figures 3.8A, B-C). MEI-1 treatment induced cytotoxicity and cell death in MCF-7 cells, with the IC_{50} value at approximately 17.33 ± 1.90 μM (Figures 3.8B, D). In contrast to MCF-7 cells, BJ fibroblast cells showed no response to MEI-1 treatment (0-50 μM) (Figures 3.8C-D), suggesting that BJ fibroblasts were more tolerant to MEI-1 treatment. Taken together, these results showed that cancer cells were more sensitive and responsive to MEI-1 treatment. In particular, the leukemia cells appeared to be most sensitive to MEI-1 treatment. Therefore, MEI-1 has the potential as an anti-cancer therapeutic agent, particularly against hematopoietic cancers (Figure 3.8D).

A)

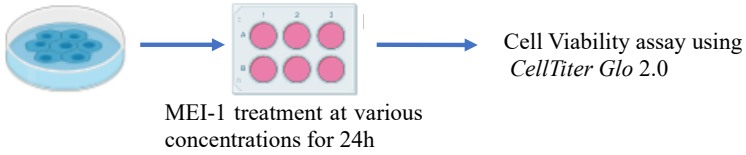

B) MCF-7

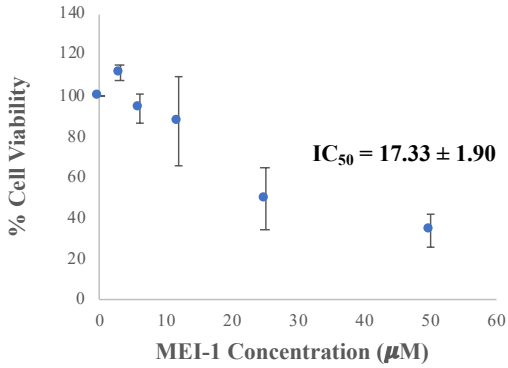

C) BJ-FB

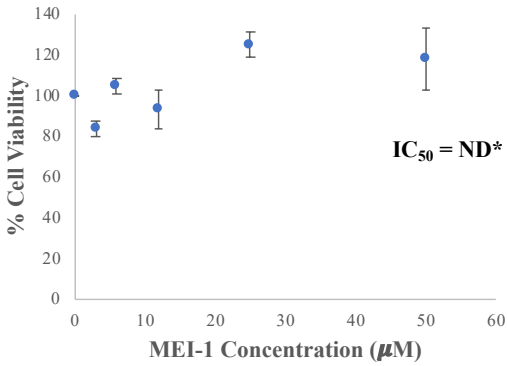

D)

Cell Line	p53 Status	IC50 Value (μM)
MCF-7	WT	17.33 ± 1.90
AML-2	WT	4.39 ± 1.16
HL-60	null	10.95 ± 0.19
HCT-116 p53 WT	WT	14.19 ± 2.04
HCT-116 p53 null	null	32.66 ± 0.31
BJ-FB	WT	ND*

Figure 3.8 (A-D): The effect of MEI-1 on cell viability in MCF-7 and BJ-FB cells. (A) Cell viability was evaluated using *CellTiter-Glo 2.0* reagent based on cellular ATP production. The figure is adapted from *Promega CellTiter-Glo 2.0 Assay Protocol.* (B-C) MCF-7 and BJ-FB cell viability under MEI-1 treatment. Three trials were conducted (N=3). Results were presented as percentage of viability and normalized against initial cell number. The IC_{50} values (μM) are represented by Mean ± SEM . (D) IC_{50} values (μM) of cell lines treated with MEI-1, including p53 status.

3.8. Purification of MDM2: MDMX RING Heterodimer through GST and His-tagged Affinity Chromatography

To examine the physical interaction between the MDM2: MDMX heterodimer and MEI-1, recombinant MDM2: MDMX RING domain heterodimer was purified. GST-tagged MDM2 RING domain (residues 417-491) was cloned in the pGEX2TK vector and the His_6-tagged MDMX RING domain (residues 416-490) was cloned in pET15b plasmid.

The recombinant MDM2: MDMX RING heterodimer was purified through dual affinity chromatography using both GST and His affinity purification. To achieve this, GST-tagged MDM2 RING domain expressed *E.coli BL21 DE3* cells were mixed with His-tagged MDMX RING domain expressed *E.coli* cells (Figure 3.9A). Through RING domain dimerization, three types of RING domain complexes would form in the cell lysate: GST-MDM2 RING homodimer, GST-MDM2: His-MDMX RING heterodimer, and His-MDMX RING homodimer. Sequential GST and Ni^{2+} affinity chromatography was used to selectively purify GST-MDM2: His-MDMX RING heterodimer. First, GST affinity chromatography could purify the GST-MDM2 RING homodimer and GST-MDM2 RING: His-MDMX RING heterodimer while removing His-MDMX RING homodimer (Figures 3.9A-B). As shown in Figure 3.9B, the elution from GST affinity chromatography contained a mixture of GST-MDM2 RING domain homodimer and GST-MDM2 RING: His-MDMX RING domain heterodimer. Ni^{2+} affinity chromatography purification was conducted next to separate the GST-MDM2: His-MDMX heterodimer from the GST-MDM2 homodimer. As shown in Figure 3.9B lanes 5 and 6, the second elution contained the purified GST-MDM2 RING: His-MDMX RING domain heterodimer. Purified recombinant MDM2: MDMX RING heterodimer was used to examine the interaction between MEI-1 and the MDM2: MDMX RING heterodimer shown in the following experiment.

A)

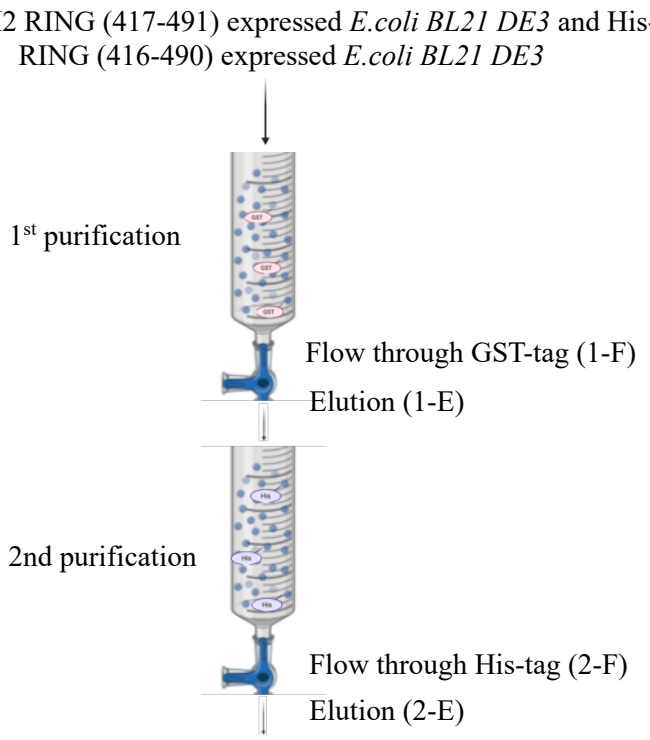

B)

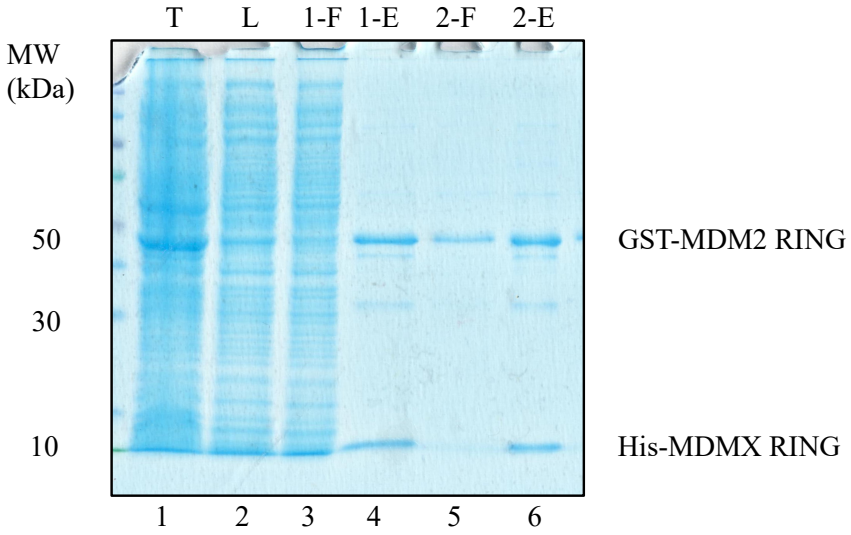

Figure 3.9 (A-B). Protein purification of recombinant MDM2: MDMX RING domain heterodimer. (A) MDM2 and MDMX RING domain homodimers were purified using sequential GST and His-tagged affinity purification. The image was created with Biorender.com (B) GST-MDM2 RING and His-MDMX RING were mixed (T) and lysed (L) together. The lysate was subject to 1st GST purification, shown in flow through (1-F) and elution (1-E). The 1st eluate was subject to 2nd Ni^{2+} affinity purification shown in flow through (2-F) and elution (2-E).

3.9. MEI-1 interacts with the MDM2: MDMX RING Heterodimer

To further examine the binary interaction between MEI-1 and the MDM2: MDMX RING heterodimer, a Biolayer Interferometry (BLI) assay was used. BLI is an optical analytical technique used to measure biomolecular interactions. This method measures the shift in the interference pattern of white light due to the change in the biological layer thickness of the biosensor tip (Wartchow et al., 2011; Duncan & Shah, 2014) (Figure 3.10A). The thickness of the biosensor tip is thus directly affected by light change and protein-protein interactions that occur. The BLI Octet assay was used to measure the association and dissociation rates of the molecular interaction between MEI-1 and MDM2: MDMX heterodimer.

As shown in Figure 3.10B step 1, a sensory probe coated with GST antibody was loaded with GST-tagged MDM2: His-tagged MDMX RING heterodimer (Figure 3.10B). MDM2: MDMX RING heterodimer was examined for physical binding with a series of increasing concentrations of MEI-1 (13 μM, 27 μM, 56 μM, 80 μM, and 126 μM) in a step wise fashion (steps 2-6) (Figure 3.10B). The baseline was established using 0 μM of MEI-1 (Figures 10B-C). Between each step, the biosensor probe was washed with buffer and re-equilibrated for new binding. There appeared to be a physical interaction between MEI-1 and the MDM2: MDMX RING heterodimer (Figures 3.10B-C). As shown in steps 2-4, increasing association followed by dissociated was observed between MDM2: MDMX and MEI-1 at concentrations of 13 μM, 27 μM and 56 μM, shown by the blue line (Figures 10B-C). The highest amount of binding was observed at 56 μM of MEI-1 (Figures 10B-C). Fitting with one-substrate binding site model, MEI-1 was shown to physically bind to the MDM2: MDMX RING heterodimer with a Kd value of 12 μM. The BLI Octet experiment was repeated under similar conditions using a His probe

and MDM2: MDMX RING heterodimer was found to bind MEI-1 with the same affinity as shown with the GST-probe (data not shown).

A)

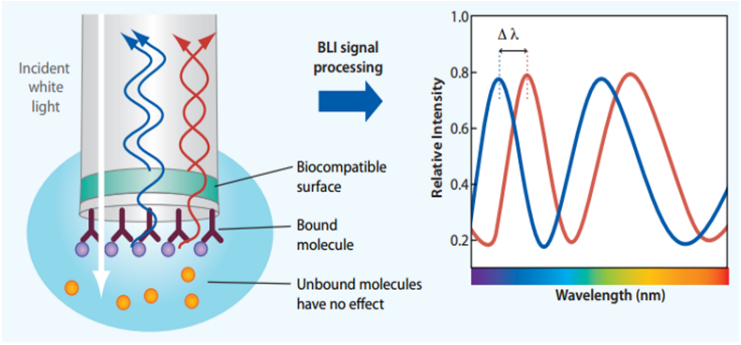

Purpose of BLI: to quantify and analyze the binding kinetics (physical interaction) of MEI-1 to MDM2:MDMX heterodimer interaction

Sensor tip surface was dipped into solution containing GST antibody. Association rate was monitored

↓

GST-tagged MDM2 His-tagged MDMX heterodimer was loaded onto sensory head

↓

Protein association and dissociation was monitored overtime by BLI signal

B)

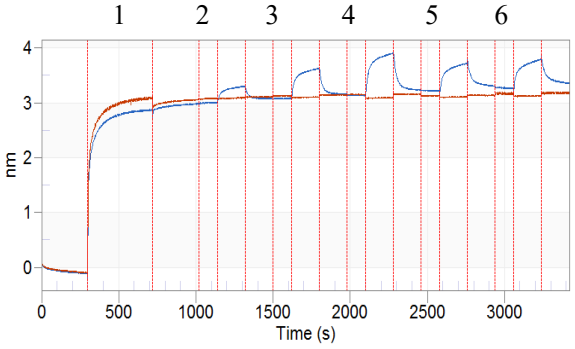

C)

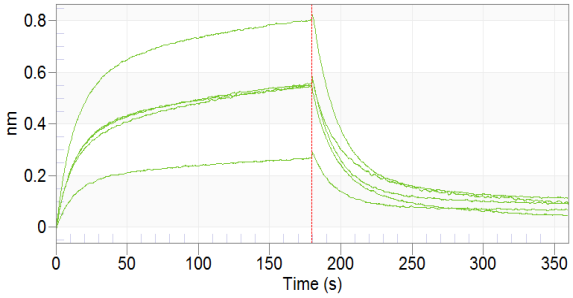

MDM2/MDMX	+	+	+	+	+	+
MEI-1 (μM)	0	13	27	56	80	126

Figure 3.10 (A-C). MEI-1 binds to the MDM2: MDMX RING domain heterodimer. (A) Schematic representation of Biolayer Interferometry (BLI) assay. The physical interaction between MEI-1 and MDM2: MDMX RING heterodimer was measured by BLI octet. The figure is adapted from *fortéBIO, handbook of surface plasmon resonance, 2nd edition (2017).* (B) The association (red line) and dissociation (blue line) between MEI-1 and MDM2: MDMX heterodimer was examined with BLI in a dose-dependent manner. GST alone was used as a control. (C) Superposition of MEI-1 association curves.

Chapter 4: Discussion

MEI-1 was identified using *in silico* docking approach as an allosteric binder to the MDM2: MDMX RING heterodimer. It was hypothesized that MEI-1 would inhibit the MDM2 RING domain and might have an effect on the overall stability of MDM2 and its other substrate proteins in cells. The purpose of this study was to validate MEI-1 as an inhibitor of MDM2 and to evaluate its anti-cancer potential. Thus, this study investigated the effect of small molecule MEI-1 in p53 wild type and p53 null leukemia and colorectal cancer cell lines to characterize cellular responses of various cancer cells to MEI-1 treatment.

MEI-1 was assessed to determine whether it had any possible anti-cancer effects through examining its cytotoxicity in cancer versus non-cancer cell lines. A cell viability assay was performed in osteosarcoma, leukemia, colorectal cancer, breast carcinoma and normal fibroblast cell lines. MEI-1 indeed induced cytotoxicity in the tested carcinogenic cells but showed little effect in BJ-FB normal cells. Among the carcinogenic cell lines used in this study, leukemia cells were found to be most sensitive to MEI-1 treatment with an inhibition constant IC_{50} value as low as 4.39 μM. In addition, colorectal and breast cancer cells also responded to MEI-1 treatment with inhibition constant values ranging from 10 – 30 μM. These results agreed with previously reported anti-cancer effects of Hinokiflavone, the chemical name for MEI-1. In previous studies, Hinokiflavone was shown to induce apoptosis and present anti-tumour activity in colorectal cancer, breast cancer, and melanoma cancer cells (Yang et al., 2018; Zhou et al., 2018; Huang et al., 2019). Thus, MEI-1 is a potential natural compound with anti-cancer effects, which could be further developed into a promising therapeutic agent to treat leukemia, osteosarcoma, breast and colorectal cancers.

Our second aim in this project was to determine if MDM2 E3 ligase activity was affected by MEI-1. Since MEI-1 was identified as a MDM2 RING domain allosteric binder, it was hypothesized that MEI-1 would inhibit MDM2-mediated ubiquitination. A previous student in the Sheng lab confirmed that MEI-1 inhibited MDM2-mediated ubiquitination in a biochemical assay. In this study, a cellular ubiquitination assay was performed in AML-2 and HL-60 leukemia cells following MEI-1 treatment. Our results concluded that MEI-1 did in fact affect MDM2 E3 ligase activity and inhibit MDM2-mediated ubiquitination. In p53 wild type leukemia cell line AML-2, MEI-1 inhibited MDM2 auto-ubiquitination and p53 ubiquitination. In HL-60 p53 null leukemia cells, MDM2 auto-ubiquitination was inhibited by MEI-1. These results agreed with the hypothesis and confirmed MEI-1's ability to inhibit MDM2 E3 ligase activity.

Cellular responses were assessed following MEI-1 treatment to determine its p53-dependent and p53-independent effects in hemopoietic cancer and colorectal cancer cell lines. It was hypothesized that MEI-1 could inhibit MDM2 to stabilize and activate p53 as a result of directly targeting the RING domain of MDM2. Furthermore, MEI-1 was also expected to stabilize additional MDM2 substrates, such as Rb and Foxo3a. To test this hypothesis, MDM2/MDMX levels in both p53 wild type and p53 null leukemia and colorectal cancer lines were evaluated by immunoblotting, following MEI-1 treatment. Interestingly, MEI-1 showed a bimodule effect on MDM2/MDMX protein levels in these cancer cell lines. A mild stabilization was seen at lower doses of MEI-1, while at greater concentrations, MEI-1 appeared to have degraded MDM2/MDMX levels. This suggests that MEI-1 inhibited MDM2 E3 ligase activity at lower concentrations, agreeing with the notion that MEI-1 targets the MDM2 RING domain. However, at higher doses, MEI-1 destabilized MDM2/MDMX proteins, although the mechanism was not

fully characterized. Since MEI-1 has been shown to bind allosterically to the MDM2: MDMX RING heterodimer interface through *in silico* structural docking analysis, MEI-1 could have a possible effect on MDM2/MDMX dimerization. This was confirmed by Shloush and colleagues with a pull-down analysis and a mutagenesis study that mutations at the dimerization interface disrupted the structural stability of the MDM2: MDMX RING heterodimer (Shloush et al., 2011). Therefore, MEI-1 is expected to affect the atomic network of the dimerization interface through binding to the MDM2: MDMX RING domain heterodimer, thereby affecting its structural stability. Thus, future studies should examine the dimerization status of the MDM2: MDMX RING domains in the presence of MEI-1. Circular Dichroism can be performed to quantify MDM2: MDMX RING heterodimer thermostability in the presence of MEI-1 and to determine if the small molecule has an effect on MDM2: MDMX RING heterodimer stability. In addition, NMR titration experiments can be performed to assess the binding interface between MEI-1 and the MDM2: MDMX RING domain.

Cellular responses were examined to explore possible effects of MEI-1 in leukemia and colorectal cancer cell lines. MEI-1 was expected to stabilize and activate p53 through the inhibition of MDM2 and induce apoptosis in a p53-dependent manner. Agreeing with this hypothesis, MEI-1 stabilized and activated p53 in leukemia and colorectal cancer cell lines. This was supported by increased levels of p53 and phosphorylated p53 at serine 15 upon MEI-1 treatment. These results suggest that MEI-1 stabilized and activated p53 by inhibiting MDM2/MDMX and confirmed MEI-1's capacity to act as an MDM2 inhibitor in a p53-dependent way. In order to further validate if MEI-1 has an effect on p53 transcriptional activity through inhibiting MDM2/MDMX, additional experiments should be conducted in these cell

lines. For instance, p53 reporter assays could be conducted following MEI-1 treatment in future experiments to evaluate the direct effect of MEI-1 on the transcriptional activity of p53. Additionally, p53 target genes such as p21, PUMA, and Noxa can be examined to show the effect of MEI-1 in p53 gene expression through assays such as quantitative real-time polymerase chain reaction (qRT-PCR), microarray, and Northern blot. Performing these experiments would provide further insight into the effect of MEI-1 on p53 signaling and transcriptional target gene expression, validating p53 activation by MEI-1.

Furthermore, leukemia and colorectal cancer cells were treated with MEI-1 to assess p53-independent MDM2 substrates. It was speculated that MEI-1 treatment would stabilize additional MDM2 substrate proteins, including Rb and Foxo3a. Indeed, Rb protein levels appeared to increase in AML-2 and HL-60 cell lines upon MEI-1 treatment. Foxo3a protein levels also exhibited a mild increase in these cell lines, suggesting that MEI-1 could affect MDM2 substrate Rb and Foxo3a stability. However, the effect of MEI-1 seemed to be cell line dependent. As seen in the colorectal cancer cells, results showed a mild or no effect in Rb and Foxo3a levels with MEI-1 treatment. Collectively, these results imply that MEI-1 could act as an MDM2 inhibitor in pathways independent of p53. Thus, it would be noteworthy to investigate other MDM2 targets, such as p21 and Nbs1, which have been shown to be directly ubiquitinated by MDM2 to further assess MEI-1 as a potential inhibitor of MDM2 (Jin et al., 2003; Zhang et al., 2004). Additionally, it would be interesting to investigate MDM2-independent pathways to explore if MEI-1 has potential anti-cancer effects independent of MDM2. Examining MEI-1's anti-cancer effects in an MDM2 knockout background would allow us to evaluate MEI-1's role in MDM2-independent pathways.

p53 is a potent activator of cellular apoptosis. MEI-1 was expected to induce apoptosis through the inhibition of MDM2, resulting in p53 activation. Two hallmarks of apoptosis, cleaved PARP and cleaved caspase-9, were used to evaluate whether MEI-1 could induce apoptosis in cancer cell lines. Our results showed that MEI-1 did in fact promote apoptotic cell death in these cancer cells. Both leukemia and colorectal cancer cell lines revealed PARP and caspase-9 cleavage at greater concentrations of MEI-1 treatment. These results were consistent with what was reported in the cell viability assay, confirming that MEI-1 exhibited anti-cancer effects through inducing apoptosis. Future studies could use flow cytometry and Annexin V experiments to further confirm that MEI-1 induced apoptosis.

This study was limited in that only apoptosis was examined as the cause of MEI-1 mediated cell death. To investigate whether MEI-1 could induce other forms of cell death, future studies should be conducted. For example, necrosis markers, including receptor-interacting serine/threonine-protein kinase 3 (RIPK3) and mixed lineage kinase domain-like (MLKL), could be used to examine the ability of MEI-1 to induce necrosis. MLKL is phosphorylated by RIPK3 and activates programmed necroptotic cell death (Yoon et al., 2017). Investigating additional markers from different forms of cell death will allow us to further explore the potential and mechanism of action of MEI-1 in inducing anti-cancer effects in cancer cells.

Two pairs of cancer cell lines were selected to examine p53 dependent and independent effects. It was hypothesized that MEI-1 would induce anti-cancer effects in both p53 wild type and p53 null cancer cells. Interestingly, cancer cell lines that were wild type for p53 were found to be more sensitive to MEI-1 treatment. Specifically, MEI-1 treatment showed a better

inhibition with lower IC_{50} values in p53 wild type cells. Moreover, MEI-1 inhibited cell proliferation more efficiently in p53 wild type compared to p53 null HCT-116 colorectal cancer cells. These results were further supported by p53 stabilization and activation observed in p53 wild type leukemia and colorectal cancer cells in MEI-1 dose dependent manner. Based on these results, it can be concluded that MEI-1 induced p53 dependent anti-cancer effects through the inhibition of MDM2. Furthermore, the anti-cancer effect of MEI-1 in the p53 null cell lines was evident from this study. MEI-1 was shown to induce cytotoxicity upon treatment and cause cellular growth inhibition in HCT-116 p53 null colorectal cancer cells. MEI-1 treatment stabilized MDM2 substrates Foxo3a and Rb, which further supported MEI-1's ability to act in a p53-independent manner. These results suggested that MEI-1 does in fact inhibit MDM2 through p53-independent pathways in carcinogenic cell lines. Anti-cancer effects of MEI-1 in p53-dependent and -independent pathways should be further assessed through additional experiments in additional carcinogenic cell lines. Animal models should be used to test MEI-1's potential as an anti-cancer therapeutic agent.

Lastly, small molecule MEI-1 was investigated to determine its binding ability to the recombinant MDM2: MDMX RING heterodimer domain. Agreeing with our initial speculation, MEI-1 did in fact bind to the MDM2: MDMX RING heterodimer. Biolayer Interferometry experiments confirmed that MEI-1 interacted with the MDM2: MDMX RING heterodimer in a dose-dependent manner. To further validate the binding of MEI-1 to its heterodimer, future work should explore the atomic details of the interaction using NMR based structural studies to map the binding between MEI-1 and MDM2: MDMX RING heterodimer and evaluate its effect on dimerization. Additionally, a mutagenesis study to mutate the binding site could be performed to

further explore the mechanism of MEI-1 binding to its RING heterodimer and its effect on MDM2 stability.

Current knowledge of existing MDM2 inhibitors in cancer therapeutics have posed numerous challenges. Nutlin-3a was shown to stimulate MDM2 overexpression as a result of p53 stabilization and initiate p53-independent tumorigenic activity of MDM2, possibly resulting in carcinogenesis. RG7112 inhibitor was discontinued as usage resulted in detrimental physiological on-site toxicities, including neutropenia and thrombocytopenia. Lastly, HLI compounds HLI98 and HLI373 were developed to inhibit MDM2 E3 ligase activity. The use of HLI98 was discontinued due its ability to induce p53-independent cellular toxicity and target additional cellular E3 ligases. The HLI373 compound remains under investigation as potential toxicities have yet to be determined. As a result of targeting the C-terminal RING domain of MDM2, it is speculated that HLI373 may lead to MDM2 and p53 stabilization, thus preventing p53 activation.

Noteworthy natural products have been successfully used in anti-cancer treatment, including plant-derived anti-cancer drugs Paclitaxel and Etoposide. Paclitaxel is derived from the Pacific yew tree, *Taxus brevifola.* It acts as a microtubule stabilizing drug that ceases cell division therefore resulting in cellular death (Weaver, B., 2014). Paclitaxel is used in breast, lung, and ovarian cancer treatment and has been approved by the FDA. Etoposide, another naturally derived anti-cancer drug, comes from podophyllotoxin, a toxin lignin that is found in the roots of Podophyllum genus plants. Etoposide inhibits DNA topoisomerase II and as a result, increases DNA cleavage (Dholwani et al., 2008). It has been used in small cell lung cancer, leukemia and

lymphoma treatments. Therefore, both Paclitaxel and Etoposide have been the front-line therapeutic drugs used in cancer treatment. MEI-1 is a naturally derived product that has the potential to inhibit MDM2 activity. MEI-1 was shown to induce anti-cancer effects in tested cancer cell lines of this study. Although this project presented insight on small molecule MEI-1, MEI-1 needs to be further explored to investigate possible toxicities overtime. As discussed, natural products, such as Paclitaxel and Etoposide play an important role in current anti-cancer therapeutics. Therefore, it would be interesting to assess naturally derived product MEI-1's potential as an anti-cancer therapeutic in cancer treatment.

Concluding Remarks

The overexpression of MDM2 has been associated with tumorigenesis and poor prognosis, which is clinically important for several human cancers, including osteosarcoma, leukemia, breast carcinoma, and colorectal cancers (reviewed in: Oliner et al., 2016; Hou et al., 2019). This study presented a small molecule, MEI-1, as a potential MDM2 inhibitor with promising anti-cancer effects in leukemia and colorectal cancer cell lines. Through cell viability assays, MEI-1 was shown to induce cell death in leukemia, breast carcinoma and colorectal cancer cell lines. Using cellular ubiquitination assays, MEI-1 was shown to inhibit MDM2 E3 ligase activity and block MDM2-mediated ubiquitination in leukemia cells. Small molecule MEI-1 was also shown to de-stabilize MDM2/MDMX and induce p53 stabilization and activation. MEI-1 also exhibited p53 independent anti-cancer effects through targeted MDM2 substrates, such as Foxo3a and Rb. Lastly, a biochemical assay revealed MEI-1's ability to physically bind with the MDM2: MDMX RING domain heterodimer.

MEI-1 is a unique MDM2 inhibitor compared to current available MDM2 antagonizers, such as Nutlin and HLI98/HLI373 compounds. Both Nutlin and HLI373 family compounds lead to MDM2 accumulation in cancer cell lines, which could be a potential oncogenic risk factor. In contrast, MEI-1 is capable of stabilizing and activating p53 while de-stabilizing MDM2 and inhibiting E3 ligase activity in cells. Thus, MEI-1 seems to be a promising MDM2 inhibitor. Whether MEI-1 could be used synergistically with Nutlin and HLI373 in cancer treatment warrants further investigation.

This project presented MEI-1 as a potential anti-cancer therapeutic agent that targets cancer cells exhibiting an overexpression of MDM2. In summary, our work contributes to a better understanding whether targeting MDM2 E3 ligase activity is a feasible anti-cancer therapeutic approach. This study provides further insight into MEI-1's role as the inhibitor of MDM2 and serves as a good framework for the future development of MEI-1 into a therapeutic agent against cancers with MDM2 overexpression.

References

AAT Bioquest, Inc. (2020, July 20). *Quest Graph™ IC50 Calculator."*. Retrieved from https://www.aatbio.com/tools/ic50-calculator

Adams, J., & Kauffman, M. (2004). Development of the proteasome inhibitor Velcade™ (Bortezomib). *Cancer Investigation*, *22*(2), 304–311. https://doi.org/10.1081/CNV-120030218

Agarwal, M. L., Agarwal, A., Taylor, W. R., & Stark, G. R. (1995). p53 controls both the G2/M and the G1 cell cycle checkpoints and mediates reversible growth arrest in human fibroblasts. *Proc. Natl. Acad. Sci. USA*, *92*, 8493–8497.

Alao, J. P. (2007). The regulation of cyclin D1 degradation: Roles in cancer development and the potential for therapeutic invention. *Molecular Cancer*, *6*. https://doi.org/10.1186/1476-4598-6-24

Alt, J. R., Bouska, A., Fernandez, M. R., Cerny, R. L., Xiao, H., & Eischen, C. M. (2005). Mdm2 Binds to Nbs1 at Sites of DNA Damage and Regulates Double Strand Break Repair. *Journal of Biological Chemistry*, *280*(19), 18771–18781. https://doi.org/10.1074/jbc.M413387200

Ardley, H. C., & Robinson, P. A. (2005). E3 ubiquitin ligases. *The Biochemical Society*, *41*, 15–30. https://doi.org/10.1042/bse0410015/853474/bse0410015.pdf

Aziz, M. H., Shen, H., & Maki, C. G. (2011). Acquisition of p53 mutations in response to the non-genotoxic p53 activator Nutlin-3. *Oncogene*, *30*(46), 4678–4686. https://doi.org/10.1038/onc.2011.185

BioRender (2020). Ubiquitin Proteasome System. Retrieved from https://app.biorender.com/biorender-templates/t-5e62661995014100889df9c2-ubiquitin-proteasome-system

Bouchard, V. J., Rouleau, M., & Poirier, G. G. (2003). PARP-1, a determinant of cell survival in response to DNA damage. *Experimental Hematology*, *31*(6), 446–454. https://doi.org/10.1016/S0301-472X(03)00083-3

Bouska, A., Lushnikova, T., Plaza, S., & Eischen, C. M. (2008). Mdm2 Promotes Genetic Instability and Transformation Independent of p53. *Molecular and Cellular Biology*, *28*(15), 4862–4874. https://doi.org/10.1128/mcb.01584-07

Bueso-Ramos, C. E., Yang, Y., Deleon, E., Mccown, P., Stass, S. A., & Albitar, M. (1993). The Human MDM-2 Oncogene Is Overexpressed in Leukemias. *Blood*, *82*(9), 2617–2623.

Burgess, A., Chia, K. M., Haupt, S., Thomas, D., Haupt, Y., & Lim, E. (2016). Clinical overview of MDM2/X-targeted therapies. *Frontiers in Oncology*, *6*, 1–7. https://doi.org/10.3389/fonc.2016.00007

Callis, J. (2014). The Ubiquitination Machinery of the Ubiquitin System. *The Arabidopsis Book*, *12*, 1–35. https://doi.org/10.1199/tab.0174

Carillo, A. M., Hicks, M., Khabele, D., & Eischen, C. M. (2015). Pharmacologically increasing Mdm2 inhibits DNA repair and cooperates with genotoxic agents to kill p53 inactivated ovarian cancer cells. *Mol Cancer Res.*, *13*(8), 1197–1205. https://doi.org/10.1016/j.gde.2016.03.011

Chen, D., Frezza, M., Schmitt, S., Kanwar, J., & Dou, Q. P. (2011). Curr Cancer Drug Targets. *Curr Cancer Drug Targets*, *11*(3), 239–253.

Chen, Y., Wang, D.-D., Wu, Y.-P., Su, D., Zhou, T. Y., Gai, R.-H., … Yang, B. (2017). MDM2 promotes epithelial-mesenchymal transition and metastasis of ovarian cancer SKOV3 cells. *British Journal of Cancer*, *117*(8), 1192–1201. https://doi.org/10.1038/bjc.2017.265

Ciechanover, A. (1994). The Ubiquitin-Proteasome Proteolytic Pathway. *Cell*, *79*, 13–21.

Danovi, D., Meulmeester, E., Pasini, D., Migliorini, D., Capra, M., Frenk, R., … Marine, J.-C. (2004). Amplification of Mdmx (or Mdm4) Directly Contributes to Tumor Formation by Inhibiting p53 Tumor Suppressor Activity. *Molecular and Cellular Biology*, *24*(13), 5835–5843. https://doi.org/10.1128/mcb.24.13.5835-5843.2004

De Bie, P., & Ciechanover, A. (2011). Ubiquitination of E3 ligases: Self-regulation of the ubiquitin system via proteolytic and non-proteolytic mechanisms. *Cell Death and Differentiation*, *18*(9), 1393–1402. https://doi.org/10.1038/cdd.2011.16

Dholwani, K., Saluja, A., Gupta, A., & Shah, D. (2008). A review on plant-derived natural products and their analogs with anti-tumor activity. *Indian Journal of Pharmacology*, *40*(2), 2–8.

Egorova, O., Lau, H. H. C., McGraphery, K., & Sheng, Y. (2020). Mdm2 and Mdmx RING domains play distinct roles in the regulation of p53 responses: A comparative study of Mdm2 and Mdmx RING domains in U2OS cells. *International Journal of Molecular Sciences*, *21*(4). https://doi.org/10.3390/ijms21041309

Egorova, O., & Sheng, Y. (2014). A site-directed mutagenesis study of the MdmX RING domain. *Biochemical and Biophysical Research Communications*, *447*(4), 696–701. https://doi.org/10.1016/j.bbrc.2014.04.065

Elmore, S. (2007). Apoptosis: A Review of Programmed Cell Death. *Toxicol Pathol.*, *35*(4), 495–516.

Espadinha, M., Barcherini, V., Lopes, E. A., & Santos, M. M. M. (2018). An Update on MDMX and Dual MDM2/X Inhibitors. *Current Topics in Medicinal Chemistry*, *18*(8), 647–660. https://doi.org/10.2174/1568026618666180604080119

Fakharzadeh, S. S., Trusko, S. P., & George, D. L. (1991). Tumorigenic potential associated with enhanced expression of a gene that is amplified in a mouse tumor cell line. *The EMBO Journal*, *10*(6), 1565–1569. https://doi.org/10.1002/j.1460-2075.1991.tb07676.x

Fang, S., Jensen, J. P., Ludwig, R. L., Vousden, K. H., & Weissman, A. M. (2000). Mdm2 Is a RING Finger-dependent Ubiquitin Protein Ligase for Itself and p53*. *THE JOURNAL OF BIOLOGICAL CHEMISTRY*, *275*(12), 8945–8951. Retrieved from http://www.jbc.org

Farhan, M., Wang, H., Gaur, U., Little, P. J., Xu, J., & Zheng, W. (2017). FOXO Signaling Pathways as Therapeutic Targets in Cancer. *International Journal of Biological Sciences*, *13*(7), 815–827. https://doi.org/10.7150/ijbs.20052

Fridman, J. S., & Lowe, S. W. (2003). Control of apoptosis by p53. *Oncogene*, *22*, 9030–9040. https://doi.org/10.1038/sj.onc.1207116

Fu, W., Ma, Q., Chen, L., Li, P., Zhang, M., Ramamoorthy, S., … Bai, W. (2009). MDM2 Acts Downstream of p53 as an E3 ligase to Promote FOXO Ubiquitination and Degradation. *Journal of Biological Chemistry*, *284*(21), 13987–14000. https://doi.org/10.1074/jbc.M901758200

Ghosh, M., Huang, K., & Berberich, S. J. (2003). Overexpression of Mdm2 and MdmX fusion proteins alters p53 mediated transactivation, ubiquitination, and degradation. *Biochemistry*, *42*(8), 2291–2299. https://doi.org/10.1021/bi0271291

Giacinti, C., & Giordano, A. (2006). RB and cell cycle progression. *Oncogene*, *25*(38), 5220–5227. https://doi.org/10.1038/sj.onc.1209615

Grice, G. L., & Nathan, J. A. (2016). The recognition of ubiquitinated proteins by the proteasome. *Cellular and Molecular Life Sciences*, *73*(18), 3497–3506. https://doi.org/10.1007/s00018-016-2255-5

Gupta, A., Shah, K., Oza, M. J., & Behl, T. (2019). Reactivation of p53 gene by MDM2 inhibitors: A novel therapy for cancer treatment. *Biomedicine and Pharmacotherapy*, *109*, 484–492. https://doi.org/10.1016/j.biopha.2018.10.155

Hannah, R., Beck, M., Moravec, R., & Riss, T. (2001). CELLTITER-GLO™ LUMINESCENT CELL VIABILITY ASSAY: A SENSITIVE AND RAPID METHOD FOR DETERMINING CELL VIABILITY. *Cell Notes*. Retrieved from www.promega.com/tbs/tb288/tb288.html

Harbour, J. W., & Dean, D. C. (2000). Rb function in cell-cycle regulation and apoptosis. *NATURE CELL BIOLOGY*, *2*. Retrieved from www.nature.com/ncb

Haupt, S., Berger, M., Goldberg, Z., & Haupt, Y. (2003). Apoptosis - The p53 network. *Journal of Cell Science*, *116*(20), 4077–4085. https://doi.org/10.1242/jcs.00739

Haupt, Y., Mayat, R., Kazazt, A., & Orent, M. (1997). letters to nature Mdm2 promotes the rapid degradation of p53. *Nature*, *387*, 296–299.

Herman, A. G., Hayano, M., Poyurovsky, M. V., Shimada, K., Skouta, R., Prives, C., & Stockwell, B. R. (2011). Discovery of Mdm2-MdmX E3 ligase inhibitors using a cell-based ubiquitination assay. *Cancer Discovery*, *1*(4), 312–325. https://doi.org/10.1158/2159-8290.CD-11-0104

Hochstrasser, M. (1995). Ubiquitin, proteasomes, and the regulation of intracellular protein degradation. *Current Opinion in Cell Biology*, *7*, 215–223.

Honda, R., & Yasuda, H. (2000). Activity of MDM2, a ubiquitin ligase, toward p53 or itself is dependent on the RING ®nger domain of the ligase. *Oncogene*, *19*, 1473–1476. Retrieved from www.nature.com/onc

Honda, R., Tanaka, H., & Yasuda, H. (1997). Oncoprotein MDM2 is a ubiquitin ligase E3 for tumor suppressor p53. *Federation of European Biochemical Societies*, *420*, 25–27.

Hou, H., Sun, D., & Zhang, X. (2019). The role of MDM2 amplification and overexpression in therapeutic resistance of malignant tumors. *Cancer Cell International*, *19*(216). https://doi.org/10.1186/s12935-019-0937-4

Huang, W., Liu, C., Liu, F., Liu, Z., Lai, G., & Yi, J. (2019). Hinokiflavone induces apoptosis and inhibits migration of breast cancer cells via EMT signalling pathway. *Cell Biochem Funct.*, 1–8.

Iwakuma, T., & Lozano, G. (2003). Subject Review MDM2, An Introduction. *Molecular Cancer Research*, *1*, 993–1000.

Jiang, L., Sheikh, M. S., & Huang, Y. (2010). Decision Making by p53: Life versus Death. *Mol Cell Pharmacol.*, *2*(2), 69–77.

Jin, Y., Lee, H., Zeng, S. X., Dai, M.-S., & Lu, H. (2003). MDM2 promotes p21waf1/cip1 proteasomal turnover independently of ubiquitination. *The EMBO Journal*, *22*(23), 6365–6377.

Jones, S. N., Hancock, A. R., Vogel, H., Donehower, L. A., & Bradley, A. (1998). Overexpression of Mdm2 in mice reveals a p53-independent role for Mdm2 in tumorigenesis. *Proc. Natl. Acad. Sci. USA*, *95*, 15608–15612.

Karni-Schmidt, O., Lokshin, M., & Prives, C. (2016). The Roles of MDM2 and MDMX in Cancer. *Annual Review of Pathology: Mechanisms of Disease*, *11*(1), 617–644. https://doi.org/10.1146/annurev-pathol-012414-040349

Kawai, H., Wiederschain, D., & Yuan, Z.-M. (2003). Critical Contribution of the MDM2 Acidic Domain to p53 Ubiquitination. *Molecular and Cellular Biology*, *23*(14), 4939–4947. https://doi.org/10.1128/mcb.23.14.4939-4947.2003

Kitagaki, J., Agama, K. K., Pommier, Y., Yang, Y., & Weissman, A. M. (2008). Targeting tumor cells expressing p53 with a water-soluble inhibitor of Hdm2. *Molecular Cancer Therapeutics*, *7*(8), 2445–2454. https://doi.org/10.1158/1535-7163.MCT-08-0063

Knudsen, E. S., & Knudsen, K. E. (2008). Tailoring to RB: Tumour suppressor status and therapeutic response. *Nature Reviews Cancer*, *8*(9), 714–724. https://doi.org/10.1038/nrc2401

Knudsen, K. E., Fribourg, A. F., Strobeck, M. W., Blanchard, J.-M., & Knudsen, E. S. (1999). Cyclin A Is a Functional Target of Retinoblastoma Tumor Suppressor Protein-mediated Cell Cycle Arrest*. *THE JOURNAL OF BIOLOGICAL CHEMISTRY*, *274*(39), 27632–27641. Retrieved from http://www.jbc.org

Kostic, M., Matt, T., Martinez-Yamout, M. A., Dyson, H. J., & Wright, P. E. (2006). Solution Structure of the Hdm2 C2H2C4 RING, a Domain Critical for Ubiquitination of p53. *Journal of Molecular Biology*, *363*(2), 433–450. https://doi.org/10.1016/j.jmb.2006.08.027

Kubbutat, M. H. G., Jones, S. N., & Vousden, K. H. (1997). Regulation of p53 stability by Mdm2. *Nature*, *387*, 299–303.

Kussie, P. H., Gorina, S., Marechal, V., Elenbaas, B., Moreau, J., Levine, A. J., & Pavletich, N. P. (1996). Structure of the MDM2 Oncoprotein Bound to the p53 Tumor Suppressor Transactivation. *Science*, *274*(5289), 948–953.

Levine, A. J. (1997). p53, the Cellular Gatekeeper Review for Growth and Division. *Cell*, *88*, 323–331.

Lindström, M. S., Jin, A., Deisenroth, C., White Wolf, G., & Zhang, Y. (2007). Cancer-Associated Mutations in the MDM2 Zinc Finger Domain Disrupt Ribosomal Protein Interaction and Attenuate MDM2-Induced p53 Degradation. *Molecular and Cellular Biology*, *27*(3), 1056–1068. https://doi.org/10.1128/mcb.01307-06

Linke, K., Mace, P. D., Smith, C. A., Vaux, D. L., Silke, J., & Day, C. L. (2008). Structure of the MDM2/MDMX RING domain heterodimer reveals dimerization is required for their ubiquitylation in trans. *Cell Death and Differentiation*, *15*(5), 841–848. https://doi.org/10.1038/sj.cdd.4402309

Maki, C. G., Huibregtse, J. M., & Howley, P. M. (1996). In Vivo Ubiquitination and Proteasome-mediated Degradation of p53. *Cancer Research*, *56*, 2649–2654.

Marine, J. C., & Lozano, G. (2010). Mdm2-mediated ubiquitylation: p53 and beyond. *Cell Death and Differentiation*, *17*(1), 93–102. https://doi.org/10.1038/cdd.2009.68

Marine, J. C. W., Dyer, M. A., & Jochemsen, A. G. (2007). MDMX: From bench to bedside. *Journal of Cell Science*, *120*(3), 371–378. https://doi.org/10.1242/jcs.03362

Marine, J. C., & Jochemsen, A. G. (2005). Mdmx as an essential regulator of p53 activity. *Biochemical and Biophysical Research Communications*, *331*(3), 750–760. https://doi.org/10.1016/j.bbrc.2005.03.151

Mendoza, M., Mandani, G., & Momand, J. (2014). The MDM2 gene family. *Biomolecular Concepts*, *5*(1), 9–19. https://doi.org/10.1515/bmc-2013-0027

Metzger, M. B., Hristova, V. A., & Weissman, A. M. (2012). HECT and RING finger families of E3 ubiquitin ligases at a glance. *Journal of Cell Science*, *125*(3), 531–537. https://doi.org/10.1242/jcs.091777

Meulmeester, E., Frenk, R., Stad, R., de Graaf, P., Marine, J.-C., Vousden, K. H., & Jochemsen, A. G. (2003). Critical Role for a Central Part of Mdm2 in the Ubiquitylation of p53. *Molecular and Cellular Biology*, *23*(14), 4929–4938. https://doi.org/10.1128/mcb.23.14.4929-4938.2003

Moll, U. M., & Petrenko, O. (2003). The MDM2-p53 Interaction. *Molecular Cancer Research*, *1*, 1001–1008.

Momand, J., Jung, D., Wilczynski, S., & Niland, J. (1998). The MDM2 gene amplification database. *Nucleic Acids Research*, *26*(15), 3453–3459. Retrieved from http://www.ncbi.nlm.nih.gov/htbin-post/Omim/dispmim?164785

Momand, J., Villegas, A., & Belyi, V. A. (2011). The evolution of MDM2 family genes. *Gene*, *486*(1–2), 23–30. https://doi.org/10.1016/j.gene.2011.06.030

Momand, J., Zambetti, G. P., Olson, D. C., George, D., & Levine', A. J. (1992). The mdm-2 Oncogene Product Forms a Complex with the ~53 Protein and Inhibits p53-Mediated Transactivation. *Cell*, *69*, 1237–1245.

Morreale, F. E., & Walden, H. (2016). Snapshot: Types of Ubiquitin Ligases. *Cell*, *165*, 1–2. https://doi.org/http://dx.doi.org/10.1016/j.cell.2016.03.003

Moududee, S. A., Jiang, Y., Gilbert, N., Xie, G., Xu, Z., Wu, J., … Shi, Y. (2018). Structural and functional characterization of hMEX-3C Ring finger domain as an E3 ubiquitin ligase. *Protein Science*, *27*(9), 1661–1669. https://doi.org/10.1002/pro.3473

Nag, S., Zhang, X., Srivenugopal, K. S., Wang, M.-H., Wang, W., & Zhang, R. (2014). Targeting MDM2-p53 Interaction for Cancer Therapy: Are We There Yet? *Curr Med Chem.*, *21*(5), 553–574.

Nomura, K., Klejnot, M., Kowalczyk, D., Hock, A. K., Sibbet, G. J., Vousden, K. H., & Huang, D. T. (2017). Structural analysis of MDM2 RING separates degradation from regulation of

p53 transcription activity. *Nature Structural and Molecular Biology*, *24*(7), 578–587. https://doi.org/10.1038/nsmb.3414

O'Keefe, K., Li, H., & Zhang, Y. (2003). Nucleocytoplasmic Shuttling of p53 Is Essential for MDM2-Mediated Cytoplasmic Degradation but Not Ubiquitination. *Molecular and Cellular Biology*, *23*(18), 6396–6405. https://doi.org/10.1128/mcb.23.18.6396-6405.2003

Oda, E., Ohki, R., Murasawa, H., Nemoto, J., Shibue, T., Yamashita, T., … Tanaka, N. (2000). Noxa, a BH3-only member of the Bcl-2 family and candidate mediator of p53-induced apoptosis. *Science*, *288*(5468), 1053–1058. https://doi.org/10.1126/science.288.5468.1053

Oliner, J. D., Kinzler, K. W., Meltzer, P. S., George, D. L., & Vogelstein, B. (1992). Amplification of a gene encoding a p53-associated protein in human sarcomas. *Nature*, *358*, 80–83.

Oliner, J. D., Pietenpol, J. A., Thiagalingam, S., Gyuris, J., Kinzler, K. W., & Vogelstein, B. (1993). Oncoprotein MDM2 conceals the activation domain of tumour suppressor p53. *Nature*, *362*, 857–860.

Oliner, J. D., Saiki, A. Y., & Caenepeel, S. (2016). The role of MDM2 amplification and overexpression in tumorigenesis. *Cold Spring Harbor Perspectives in Medicine*, *6*(6). https://doi.org/10.1101/cshperspect.a026336

Oliver, F. J., De La Rubia, G., Ronique Rolli, V., Carmen Ruiz-Ruiz, M., De Murcia, G., & Ménissier-De Murcia, J. (1998). Importance of Poly(ADP-ribose) Polymerase and Its Cleavage in Apoptosis. *THE JOURNAL OF BIOLOGICAL CHEMISTRY*, *273*(50), 33533–33539. Retrieved from http://www.jbc.org/

Olivier, M., Hollstein, M., & Hainaut, P. (2010). TP53 mutations in human cancers: origins, consequences, and clinical use. *Cold Spring Harbor Perspectives in Biology*, *2*(1). https://doi.org/10.1101/cshperspect.a001008

Ozaki, T., & Nakagawara, A. (2011). Role of p53 in cell death and human cancers. *Cancers*, *3*(1), 994–1013. https://doi.org/10.3390/cancers3010994

Pan, Y., & Chen, J. (2003). MDM2 Promotes Ubiquitination and Degradation of MDMX. *Molecular and Cellular Biology*, *23*(15), 5113–5121. https://doi.org/10.1128/mcb.23.15.5113-5121.2003

Pazgier, M., Liu, M., Zou, G., Yuan, W., Li, C., Li, C., … Lu, W. (2009). Structural basis for high-affinity peptide inhibition of p53 interactions with MDM2 and MDMX. *PNAS*, *106*(12), 4665–4670.

Perri, F., Pisconti, S., & Vittoria Scarpati, G. Della. (2016). P53 mutations and cancer: A tight linkage. *Annals of Translational Medicine*, *4*(24). https://doi.org/10.21037/atm.2016.12.40

Picksley, S. M., & Lane, D. P. (1993). The p53-mdm2 Autoregulatory Feedback Loop: A Paradigm for the Regulation of Growth Control by p53? *BioEssays*, *15*(10), 689–690.

Polager, S., & Ginsberg, D. (2009). p53 and E2f: partners in life and death. *Nature Reviews*, *9*, 738–748.

Poyurovsky, M. V., Priest, C., Kentsis, A., Borden, K. L. B., Pan, Z. Q., Pavletich, N., & Prives, C. (2007). The Mdm2 RING domain C-terminus is required for supramolecular assembly and ubiquitin ligase activity. *EMBO Journal*, *26*(1), 90–101. https://doi.org/10.1038/sj.emboj.7601465

Prives, C., & Hall, P. A. (1999). The p53 Pathway. *J. Pathol*, *187*, 112–126. Retrieved from http://perso.curie.fr/Thierry.Soussi/index.html

Proctor, C. J., & Gray, D. A. (2008). Explaining oscillations and variability in the p53-Mdm2 system. *BMC Systems Biology*, *2*(2006), 1–20. https://doi.org/10.1186/1752-0509-2-75

Ranaweera, R. S., & Yang, X. (2013). Auto-ubiquitination of Mdm2 enhances its substrate ubiquitin ligase activity. *Journal of Biological Chemistry*, *288*(26), 18939–18946. https://doi.org/10.1074/jbc.M113.454470

Scheffner, M., Nuber, U., & Hulbregtse, J. M. (1995). Protein ubiquitination involving an E1-E2-E3 enzyme ubiquitin thioester cascade. *14. Seufert, W. & Jentsch, S. EMBO J*, *248*(6), 1773–1784.

Schrader, E. K., Harstad, K. G., & Matouschek, A. (2009). Targeting proteins for degradation. *Nature Chemical Biology*, *5*(11), 815–822. https://doi.org/10.1038/nchembio.250

Senturk, E., & Manfredi, J. J. (2013). p53 and Cell Cycle Effects After DNA Damage. *Methods Mol Biol.*, *962*, 49–61. https://doi.org/10.1007/978-1-62703-236-0_4

Shadfan, M., Lopez-Pajares, V., & Yuan, Z.-M. (2012). MDM2 and MDMX: Alone and together in regulation of p53. *Transl Cancer Res.*, *1*(2), 88–89.

Shah, N. B., & Duncan, T. M. (2014). Bio-layer interferometry for measuring kinetics of protein-protein interactions and allosteric ligand effects. *Journal of Visualized Experiments*, *84*, 1–7. https://doi.org/10.3791/51383

Shasfoort, R. (2017). *fortébio, HANDBOOK OF SURFACE PLASMON RESONANCE, 2ND EDITION.* DOI: 10.1039/9781847558220.

Shloush, J., Vlassov, J. E., Engson, I., Duan, S., Saridakis, V., Dhe-paganon, S., … Arrowsmith, C. H. (2011). Structural and functional comparison of the RING domains of two p53 E3 ligases, Mdm2 and Pirh2. *Journal of Biological Chemistry*, *286*(6), 4796–4808. https://doi.org/10.1074/jbc.M110.157669

Shvarts, A., Bazuine, M., Dekker, P., Ramos, Y. F. M., Steegenga, W. T., Merckx, G., … Jochemsen, A. G. (1997). Isolation and Identification of the Human Homolog of a New p53-Binding Protein, Mdmx. *Genomics*, *43*, 34–32. Retrieved from http://hdl.handle.net/2066/26148

Shvarts, A.T., Steegenga, W., Riteco, N., van Laar, T., Dekker, P., Bazuine, M., … Jochemsen, A. G. (1996). MDMX: a novel p53-binding protein with some functional properties of MDM2. *The EMBO Journal*, *15*(19), 5349–5357.

Soengas, M. S., Capodieci, P., Polsky, D., Mora, J., Esteller, M., Opitz-Araya, X., … Lowe, S. W. (2001). Inactivation of the apoptosis effector Apaf-1 in malignant melanoma. *Nature*, *409*.

Spratt, D. E., Walden, H., & Shaw, G. S. (2014). RBR E3 ubiquitin ligases: New structures, new insights, new questions. *Biochemical Journal*, *458*(3), 421–437. https://doi.org/10.1042/BJ20140006

Stewart, M. D., Ritterhoff, T., Klevit, R. E., & Brzovic, P. S. (2016). E2 enzymes: More than just middle men. *Cell Research*, *26*(4), 423–440. https://doi.org/10.1038/cr.2016.35

Tisato, V., Voltan, R., Gonelli, A., Secchiero, P., & Zauli, G. (2017). MDM2/X inhibitors under clinical evaluation: Perspectives for the management of hematological malignancies and pediatric cancer. *Journal of Hematology and Oncology*, *10*(1). https://doi.org/10.1186/s13045-017-0500-5

Titia, L., Linares, K., Hengstermann, A., Ciechanover, A., Mü Ller ‡, S., & Scheffner, M. (2003). HdmX stimulates Hdm2-mediated ubiquitination and degradation of p53. *PNAS*, *100*(21), 12009–12014. Retrieved from www.pnas.orgcgidoi10.1073pnas.2030930100

Vassilev, L. T., Vu, B. T., Graves, B., Carvajal, D., Podlaski, F., Filipovic, Z., … Liu, E. A. (2004). In Vivo Activation of the p53 Pathway by Small-Molecule Antagonists of MDM2. *Science*, *303*(5659), 844–848. https://doi.org/10.1126/science.1092472

Verma, R., Rigatti, M. J., Belinsky, G. S., Godman, C. A., & Giardina, C. (2010). DNA damage response to the Mdm2 inhibitor Nutlin-3. *Biochem Pharmacol.*, *79*(4), 564–574. https://doi.org/10.1038/jid.2014.371

Vousden, K. H., & Nakano, K. (2001). PUMA, a Novel Proapoptotic Gene, Is Induced by p53. *Molecular Cell*, *7*, 683–694.

Wade, M., Wang, Y. V., & Wahl, G. M. (2010). The p53 orchestra: Mdm2 and Mdmx set the tone. *Trends in Cell Biology*, *20*(5), 299–309. https://doi.org/10.1016/j.tcb.2010.01.009

Wang, B., Wu, S., Liu, J., Yang, K., Xie, H., & Tang, W. (2019). Development of selective small molecule MDM2 degraders based on nutlin. *European Journal of Medicinal Chemistry*, *176*, 476–491. https://doi.org/10.1016/j.ejmech.2019.05.046

Wang, W., Zhang, X., Qin, J. J., Voruganti, S., Nag, S. A., Wang, M. H., … Zhang, R. (2012). Natural product Ginsenoside 25-OCH3-PPD Inhibits Breast Cancer Growth and Metastasis through Down-Regulating MDM2. *PLoS ONE*, *7*(7). https://doi.org/10.1371/journal.pone.0041586

Wartchow, C. A., Podlaski, F., Li, S., Rowan, K., Zhang, X., Mark, D., & Huang, K.-S. (2011). Biosensor-based small molecule fragment screening with biolayer interferometry. *Journal of Computer-Aided Molecular Design*, *25*(7), 669–676. https://doi.org/10.1007/s10822-011-9439-8

Weaver, B. A. (2014). How Taxol / paclitaxel kills cancer cells. *Molecular Biology of the Cell*, *25*, 2677–2681. https://doi.org/10.1091/mbc.E14-04-0916

Wienken, M., Moll, U. M., & Dobbelstein, M. (2017). Mdm2 as a chromatin modifier. *Journal of Molecular Cell Biology*, *9*(1), 74–80. https://doi.org/10.1093/jmcb/mjw046

Wu, X., Bayle, J. H., Olson, D., & Levine, A. J. (1993). The p53-mdm-2 autoregulatory feedback loop. *Genes & Development*, *7*, 1126–1132.

Xiao, Z.-X., Chen, J., Levine, A. J., Modjtahedl, N., Xing, J., Sellers, W. R., & Livingston, D. M. (1995). Interaction between the retinoblastoma protein and the oncoprotein MDM2. *Nature*, *375*, 694–698.

Yang, H.-Y., Wen, Y.-Y., Chen, C.-H., Lozano, G., & Lee, M.-H. (2003). 14-3-3σ Positively Regulates p53 and Suppresses Tumor Growth. *Molecular and Cellular Biology*, *23*(20), 7096–7107. https://doi.org/10.1128/mcb.23.20.7096-7107.2003

Yang, J. Y., Zong, C. S., Xia, W., Yamaguchi, H., Ding, Q., Xie, X., … Hung, M. C. (2008). ERK promotes tumorigenesis by inhibiting FOXO3a via MDM2-mediated degradation. *Nature Cell Biology*, *10*(2), 138–148. https://doi.org/10.1038/ncb1676

Yang, S., Zhang, Y., Luo, Y., Xu, B., Yao, Y., Deng, Y., … Xie, Y. (2018). Hinokiflavone induces apoptosis in melanoma cells through the ROS-mitochondrial apoptotic pathway and impairs cell migration and invasion. *Biomedicine and Pharmacotherapy*, *103*, 101–110. https://doi.org/10.1016/j.biopha.2018.02.076

Yang, W., Dolloff, N. G., & El-Deiry, W. (2008). ERK and MDM2 prey on FOXO3a. *Nature Cell Biology*, *10*(2), 125–126.

Yang, Y., Kitagaki, J., Wang, H., Hou, D. X., & Perantoni, A. O. (2009). Targeting the ubiquitin-proteasome system for cancer therapy. *Cancer Science*, *100*(1), 24–28. https://doi.org/10.1111/j.1349-7006.2008.01013.x

Yang, Y., Ludwig, R. L., Jensen, J. P., Pierre, S. A., Medaglia, M. V., Davydov, I. V., … Vousden, K. H. (2005). Small molecule inhibitors of HDM2 ubiquitin ligase activity

stabilize and activate p53 in cells. *Cancer Cell*, *7*(6), 547–559. https://doi.org/10.1016/j.ccr.2005.04.029

Yoon, S., Kovalenko, A., Bogdanov, K., & Wallach, D. (2017). MLKL, the Protein that Mediates Necroptosis, Also Regulates Endosomal Trafficking and Extracellular Vesicle Generation. *Immunity*, *47*(1), 51–65. https://doi.org/10.1016/j.immuni.2017.06.001

Zhang, Q., Zeng, S. X., & Lu, H. (2014). Targeting p53-MDM2-MDMX loop for cancer therapy. *Sub-Cellular Biochemistry*, *85*, 281–319. https://doi.org/10.1007/978-94-017-9211-0_16

Zhang, X., Tang, N., Hadden, T. J., & Rishi, A. K. (2011). Akt, FoxO and regulation of apoptosis. *Biochimica et Biophysica Acta - Molecular Cell Research*, *1813*(11), 1978–1986. https://doi.org/10.1016/j.bbamcr.2011.03.010

Zhang, Z., Wang, H., Li, M., Agrawal, S., Chen, X., & Zhang, R. (2004). MDM2 Is a Negative Regulator of p21WAF1/CIP1, Independent of p53. *Journal of Biological Chemistry*, *279*(16), 16000–16006. https://doi.org/10.1074/jbc.M312264200

Zhou, J., Zhao, R., Ye, T., Yang, S., Li, Y., Yang, F., … Li, Q. (2019). Antitumor activity in colorectal cancer induced by hinokiflavone. *Journal of Gastroenterology and Hepatology (Australia)*, *34*(9), 1571–1580. https://doi.org/10.1111/jgh.14581

Zhu, L. (2005). Tumour suppressor retinoblastoma protein Rb: A transcriptional regulator. *European Journal of Cancer*, *41*(16), 2415–2427. https://doi.org/10.1016/j.ejca.2005.08.009

Appendix

Table 1: AML-2 and HL-60 cell viability statistical analysis

Concentration (μM)	AML-2 (Mean ± SEM)	HL-60 (Mean ± SEM)
0	100 ± 0.00	100 ± 0.00
3	62 ± 0.03	103 ± 0.06
6	22 ± 0.01	84 ± 0.04
12	7 ± 0.01	42 ± 0.03
25	1 ± 0.00	2 ± 0.00

Table 2: HCT-116 p53 WT and HCT-116 p53 null cell viability statistical analysis

Concentration (μM)	HCT-116 p53 WT (Mean ± SEM)	HCT-116 p53 Null (Mean ± SEM)
0	100 ± 0.00	100 ± 0.00
6	44 ± 0.00	80 ± 0.00
12	36 ± 0.00	72 ± 0.00
25	24 ± 0.00	54 ± 0.00
50	15 ± 0.00	25 ± 0.00
100	7 ± 0.00	13 ± 0.00

Table 3: MCF-7 and BJ-FB cell viability statistical analysis

Concentration (μM)	MCF-7 (Mean ± SEM)	BJ-FB (Mean ± SEM)
0	100 ± 0.00	100 ± 0.00
3	111 ± 0.02	84 ± 0.02
6	93 ± 0.04	104 ± 0.02
12	87 ± 0.13	93 ± 0.06
25	49 ± 0.09	125 ± 0.04
50	34 ± 0.05	118 ± 0.09

Appendix A. Cell viability statistical analysis of cancer and non-cancer cell lines at various concentrations of MEI-1. Three trials were conducted (N=3) for each cell line. Cell viability was quantified at each MEI-1 concentration (μM) and represented by percentage of viable cells normalized with cells without MEI-1 treatment. Cell viability were shown as percentage (%) of Mean ± SEM for each concentration tested.